

Review

Not peer-reviewed version

From Nature to Technology: Exploring Bioinspired Polymer Actuators via Electrospinning

[Muhammad Yasar Razzag](#)^{*}, [Maria Balk](#)^{*}, [Magdalena Mazurek-Budzyńska](#)^{*}, Anke Schadewald

Posted Date: 25 August 2023

doi: 10.20944/preprints202308.1771.v1

Keywords: electrospinning; bioinspired actuators; stimuli-sensitive hydrogels; shape-memory polymers (SMP); electroactive polymers



Preprints.org is a free multidiscipline platform providing preprint service that is dedicated to making early versions of research outputs permanently available and citable. Preprints posted at Preprints.org appear in Web of Science, Crossref, Google Scholar, Scilit, Europe PMC.

Copyright: This is an open access article distributed under the Creative Commons Attribution License which permits unrestricted use, distribution, and reproduction in any medium, provided the original work is properly cited.

Review

From Nature to Technology: Exploring Bioinspired Polymer Actuators via Electrospinning

Muhammad Yasar Razzaq^{1,*}, Maria Balk^{2,*}, Magdalena Mazurek-Budzyńska^{3,*} and Anke Schadewald¹

¹ Institut für Kunststofftechnologie und Recycling e. V., D-6369 Weißandt-Gölzau, Germany

² Institute of Active Polymers, Helmholtz-Zentrum Hereon, D-14513 Teltow, Germany

³ Department of Chemistry, Warsaw University of Technology, Warsaw, Poland

* Correspondence: yasar.razzaq@iktr-online.de (M.Y.R.); maria.balk@hereon.de (M.B.); magdalena.budzynska@pw.edu.pl (M.M.-B.)

Abstract: Nature has always been a source of inspiration for the development of novel materials and devices. In particular, polymer actuators that mimic the movements and functions of natural organisms have been of great interest due to their potential applications in various fields, such as biomedical engineering, soft robotics, and energy harvesting. During recent years, the development and actuation performance of electrospun fibrous meshes with the advantages of high permeability, surface area and easy functional modification, has received extensive attention from researchers. This review covers the recent progress in the state-of-the-art electrospun actuators based on commonly used polymers such as stimuli-sensitive hydrogels, shape-memory polymers (SMPs), and electroactive polymers. The design strategies inspired by nature such as hierarchical systems, layered structures, responsive interfaces to enhance the performance, and functionality of these actuators including the role of biomimicry to create devices that mimic the behavior of natural organism are discussed. Finally, the challenges and future directions in the field, with a focus on the development of more efficient and versatile electrospun polymer actuators that can be used in a wide range of applications, are addressed. The insights gained from this review can contribute to the development of advanced and multifunctional actuators with improved performance and expanded application possibilities.

Keywords: electrospinning; bioinspired actuators; stimuli-sensitive hydrogels; shape-memory polymers (SMP); electroactive polymers

1. Introduction

Nature has long served as a boundless source of inspiration for scientists and engineers seeking to develop innovative technologies. The realm of bio inspiration, specifically, aims to emulate and harness the extraordinary capabilities observed in biological systems [1,2]. One area of particular interest in biomimetics is the development of polymer actuators inspired by nature [3]. Polymer actuators can convert electrical, thermal, or chemical energy into mechanical motion. They are composed of polymeric materials that can undergo significant changes in shape, size, or stiffness in response to a stimulus. This unique property makes them ideal for use in a wide range of applications, including (soft) robotics, biomedical devices, energy harvesting systems, and artificial muscles [4–6]. A well-known example of a bioinspired actuator is the artificial muscle, which aims to replicate the contractile behavior of natural muscles. Natural muscles are composed of a network of protein fibers that can slide past one another to generate force and motion [7]. Other examples of natural actuations that have inspired material scientist include the movement of plant tendrils [8] and the morphing of butterfly wings [9]. Tendrils are able to wrap around support structures by combining changes in turgor pressure with differential growth, while butterfly wings can change their colour and shape through the controlled movement of scales and ridges [10,11].

Researchers have developed various bioinspired polymer actuators (BiPA) with unique properties and based on various smart polymers such as stimuli-sensitive hydrogels, shape-memory polymers (SMPs) or electroactive polymers (EAP) [12–15]. One of the most notable features of these materials is their ability to undergo large, rapid changes in shape and size in response to stimuli such as temperature, humidity, light, or electric fields [5,6,16–19]. For instance, stimuli-sensitive hydrogels are hydrophilic polymer networks and exhibit large volume changes, leading to shape transformations or the generation of mechanical work by exposure to different stimuli [6,20,21]. SMPs are another fascinating class of smart materials, which possess the ability to undergo substantial deformation when subjected to an external stimulus such as heat, light or pH change, and subsequently, recover their original shape upon exposure to a triggering stimulus [17,22–25]. EAP, in contrast to SMPs, have the ability to deform under the influence of an electric field, and are attractive for a wide range of applications including robotics, biomedical devices, haptic interfaces, and microelectromechanical systems (MEMS) [13,26,27]. Overall, the synthesis of these intelligent polymer materials, the integration of multi-responsive functionalities, and the progress in fabrication techniques have significantly expanded their capabilities and performance.

In addition to their responsive properties, stimuli-sensitive polymers can also exhibit remarkable strength, flexibility, and durability [11,18,28–30]. This makes them highly desirable for applications such as soft robotics and wearable devices, where flexibility and durability are key requirements [31]. In recent years, significant advancements have been made in the synthesis, characterization, and application of these smart polymers, propelling them into exciting new territories. However, despite the many promising features of BiPA, there are also significant challenges associated with their development and use. For example, the design and fabrication of these materials require careful consideration of factors such as scalability, biocompatibility, and stability over time. Additionally, there is a need for improved characterization techniques and theoretical models that can accurately predict the behaviour of these complex materials [18,31–33].

Electrospinning is a widely used technique for fabricating polymeric fibrous meshes, as it allows for precise control over the fiber diameter and alignment, as well as the incorporation of various functional components (Figure 1) [34,35]. The use of nature as a source of inspiration for the design of electrospun polymer actuators has led to the development of devices that can replicate the movements and functions of natural organisms. For example, some electrospun polymer actuators have been designed to mimic the movements of muscle fibers [36], while others have been inspired by the motion of insects, plants, or other organisms. By controlling the parameters of electrospinning, such as the solution viscosity, flow rate, and applied voltage, it is possible to tune the morphology and mechanical properties of the resulting fibers [37]. One of the advantages of electrospun polymer actuators is their ability to exhibit multiple functions, such as responding to various stimuli and performing multiple tasks such as locomotion, sensing, colour changing etc. [38]. Moreover, electrospinning can be combined with other techniques such as 3D printing and microfabrication to create complex and functional structures.

As the field of bioinspired electrospun actuators continues to expand, several challenges and opportunities lie ahead. This paper will review the current advancements, fabrication techniques, and actuation mechanisms of electrospun hydrogels-based actuators, SMPs, and EAP, while also discussing the limitations and potential solutions to overcome them. By presenting an overview of the latest research, this paper aims to inspire and guide researchers in their pursuit of bioinspired polymer actuators, fostering a deeper understanding of the synergistic relationship between nature and engineering and unlocking new frontiers in the development of next-generation actuation technologies.

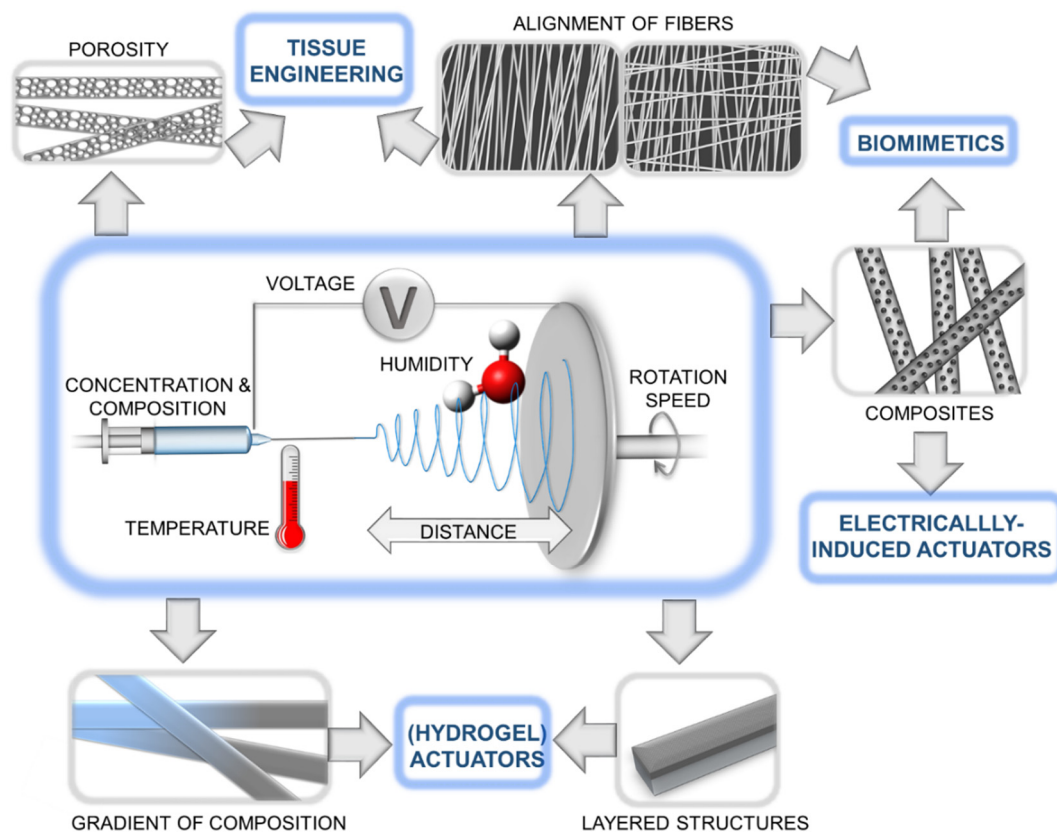


Figure 1. Schematic illustration of electrospinning process along with various architectures of electrospun fibers and potential applications.

The review also highlights the potential applications of electrospun polymer actuators, including drug delivery, tissue engineering, and soft robotics. Finally, the challenges and future directions in the field of electrospun BiPA inspired by nature will be discussed. These challenges include improving the efficiency and controllability of these devices, as well as expanding their potential applications in different fields. Overall, this review provides a comprehensive overview of the current state of the art in this exciting field and highlights the potential for the development of new and innovative fiber based polymer actuators inspired by nature.

2. Biomimetic inspiration for synthetic actuators

Biological systems, honed by millions of years of evolution, offer an extraordinary repertoire of intricate and adaptive movements that have inspired the development of cutting-edge synthetic actuators. As researchers delve deeper into the mechanisms governing stimuli-sensitive locomotion and movements in living organisms, they have uncovered fascinating adaptations that not only showcase remarkable performance but also unparalleled energy efficiency [14,30]. For instance, animals rely on muscle contractions for various movements, such as walking, flying, and swimming [39]. Muscles are composed of bundles of specialized fibers called myofibrils, which are made up of proteins called actin and myosin. When stimulated by electrical signals from the nervous system, actin and myosin interact, causing the myofibrils to contract and generate force. This contraction allows organisms to produce a wide range of reversible movements, such as walking, grasping, or flexing muscles [40,41]. Tendons and ligaments are fibrous connective tissues that attach muscles to bones (tendons) and bones to other bones (ligaments) (Figure 2a). They are primarily composed of collagen fibers, which provide strength and flexibility. Tendons transmit forces from muscle contractions to bones, allowing movement at joints, while ligaments provide stability and limit joint movements to prevent excessive strain [42]. Marine invertebrates, possess specialized fibrous structures that enable reversible movements. For example, certain types of tentacles in jellyfish or

anemones contain fibrous proteins that can rapidly extend or contract, allowing these organisms to capture prey or withdraw from potential threats [43]. Tropic or nastic responses in plants enable directional growth or movements to adopt new environments. For instance, tropic response includes phototropism, which is the movement of plants in response to light. Photoreceptor cells, such as phytochromes and phototropins, sense the light intensity [44] and direction, thus triggering differential growth in various parts of the plants [45].

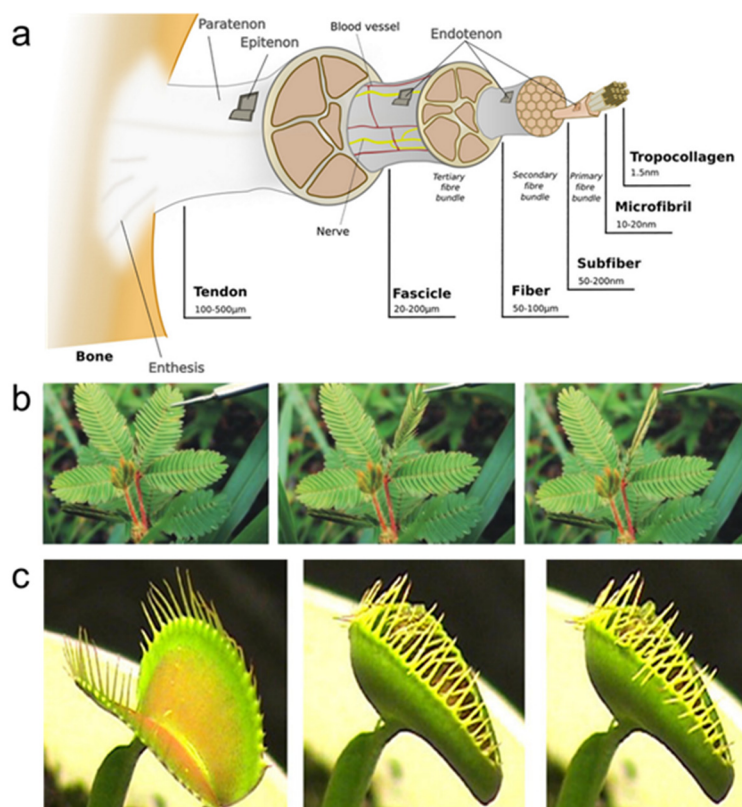


Figure 2. Representative actuating structures in living systems (a) Hierarchical structure of the tendon/ligament. The tropocollagen cross-linked molecules are arranged in microfibrils, subfibrils, fibrils, fibers, and fascicles. Reprinted from [45], Copyright 2021, with permission from Elsevier. (b) Touch induced folding/unfolding of mimosa leaflets. Reprinted from [43], Copyright 2011, with permission from Taylor & Francis. (c) The snap-trap of the carnivorous Venus flytrap (*D. muscipula*) closes after the mechanical triggering of sensitive hairs, leading to a swift concave-convex curvature change of the two trap lobes. Reprinted from [46], Copyright 2011, with permission from Elsevier.

Climbing plants, like vines, employ thigmotropism to sense and respond to physical contact [47]. They possess specialized fibrous structures, such as tendrils, which wrap around support structures when they come into contact with them [48]. By doing so, these plants can grow and climb upward, utilizing external structures for stability and support. The nastic movements in plants are reversible, non-directional responses to external stimuli that result in changes in the orientation of plant organs e.g., rapid folding or drooping of leaves in the sensitive plant (*Mimosa pudica*) when touched. These movements are facilitated by specialized filaments or fibrous tissues within the plant structures, which undergo reversible changes in turgor pressure or cell elongation [44]. Another example is seismonastic movements that occur in response to vibrations or mechanical disturbances e.g., Venus flytrap, which closes its leaves rapidly when triggered by the movement of an insect [49]. There are tiny hairs at the edges of the leaves which act as mechanosensors and traps the insect by generating an electrical signal [50]. Some of the representative actuations in living systems are shown in Figure 2. The adaptability and responsiveness of living systems to different stimuli, which not only significantly enhance their survival abilities but also provide inspirations for the design of

bioinspired actuators capable of responding to a range of stimuli, opening doors to innovative applications in robotics, materials science, and biomedical engineering [1,14,28].

3. Electrospun hydrogel actuators

Many natural and artificial materials can show swelling and shrinkage behavior by responding to changes in environmental humidity. As examples, the skin of the human hands and feet forms wrinkles upon continued submersion in water [51] and pine cones can exhibit a folded shape on rainy days and an open shape when it is dry [52]. Especially in case of pine cones, the motion relies on a bilayered structure of the individual scales that can change their conformation when the humidity is increased/decreased [53].

This phenomenon inspired the design of bilayer hydrogel actuators, in which one of the layers (called the active layer) can change its volume by means of swelling / deswelling effects [21]. The second layer (called the passive layer) is inert to the dimensional change. A macroscopic shape shift can be obtained as result of generated stresses at the interface of the two layers. The resulting movements can be controlled by the variation of material types, thickness, mechanical characteristics in the bilayer system, sample size, and geometry. Electrospun hydrogel actuators often based on thermo-responsive polymers (e.g., poly(*N*-isopropylacrylamide)—PNIPAM), which can uptake or release water as function of temperature based on a phase separation upon heating (lower critical solution temperature—LCST) [54,55]. Although organic solvent-based synthetic actuators are described in literature, water based systems are of importance as water is highly relevant for living systems and allows biomedical applications [18]. Hence, the research on electrospun actuator materials is also focusing on hydrogel based systems.

3.1. Water-, temperature-, light-, and electric field-responsive hydrogel actuators

Electrospun hydrogels based on the copolymer of thermo-responsive NIPAM with a photoreactive 4-acryloylbenzophenone (ABP)—conjugated comonomer provide a temperature triggered swelling/deswelling response with increasing/decreasing sample volume [20]. The created crosslinked copolymer mats showed a rapid swelling behavior in an aqueous environment with a water content > 60 wt%. As result of the LCST of PNIPAM, aggregates based on hydrogen bondings as additional temporary crosslinks can be created in hot water (deswelling). The prepared fibrous hydrogels showed a fast thermal response and a rapid self-recovery (74% within 10 s) after loading–unloading tensile cycles in water. Besides changes of material volume, real reversible movements were reported by a humidity-responsive bilayer actuator, which was created by combining an electrospun polyvinylpyrrolidone (PVP)/poly(acrylic acid) (PAA) active layer with a polyimide film as passive layer [56]. This actuator showed bending movements when humidity was increased as result of swelling within the active layer and the created stress mismatch for the bilayer system. In this case, the properties of the active layer changed during actuation between a swollen hydrogel and a non-swollen polymeric layer, which presents the simplest concept for the design of reversible movements for electrospun hydrogel actuators. In contrast to that, soft actuators were designed, in which the active layer is swollen during the whole actuation cycle. Here, hydrogels with a super-fast actuation behavior of less than one second were demonstrated by bilayer nanofiber mats made by sequential electrospinning and subsequent photo-crosslinking of the thermo-responsive polymer P(NIPAM-ABP) (active layer) and thermoplastic polyurethane (TPU—passive layer) [57]. A macroscopic shape shift was realized in warm water (40 °C) and the restoration of sample shape in cold water (4 °C). By means of self-folding triggered by temperature changes, 3D structures could be obtained.

The bending movement for electrospun soft actuators can be adjusted by variation of the thickness of the different layers in bilayer structures as demonstrated for PNIPAM and cellulose nanocrystals (CNCs) based actuators [58]. The two layers included different amounts of CNCs, whereby the water uptake upon heating and cooling was influenced (decreased swelling with increasing CNCs content). A 3D geometry was obtained when the bilayer system came into contact with water for the first time via anisotropic swelling of the two layers. Reversible shape shifts were

observed by subsequent swelling / deswelling as a result of temperature changes between 20 °C and 40 °C. More interestingly, also the direction of macroscopic shape shifts can be controlled. As example, reversible shape shifts could be realized by means of a fibrous bilayer system with TPU (as passive layer) and crosslinked PNIPAM fibers (as an active layer) [59]. Here, the angle of fiber orientation controlled the direction of reversible movements. The bilayers were developed by sequential electrospinning of TPU with ABP as photo crosslinker and of the thermo-responsive PNIPAm with ABP. The direction of actuation behavior was adjusted by cutting the bilayer systems at different angles (0°-fibers oriented parallel to the long axis; 90°-fibers oriented perpendicular to the long axis; 45°-fibers oriented 45° to the long axis). The asymmetric swelling (at 4 °C)/shrinking (at 40 °C) of hydrogel fibers as result of temperature changes induced the creation of different shapes and the high porosity of the bilayer system enabled a fast actuation (Figure 3). As alternative to that, the combination of electrospinning of a thermo-responsive PNIPAM membrane and 3D printing of different well-designed PNIPAm/clay patterns on the electrospun membranes enables that the created internal stresses generated by swelling / deswelling effects can be guided [60]. Hence, complex shape geometries with controlled shape shifts could be obtained.

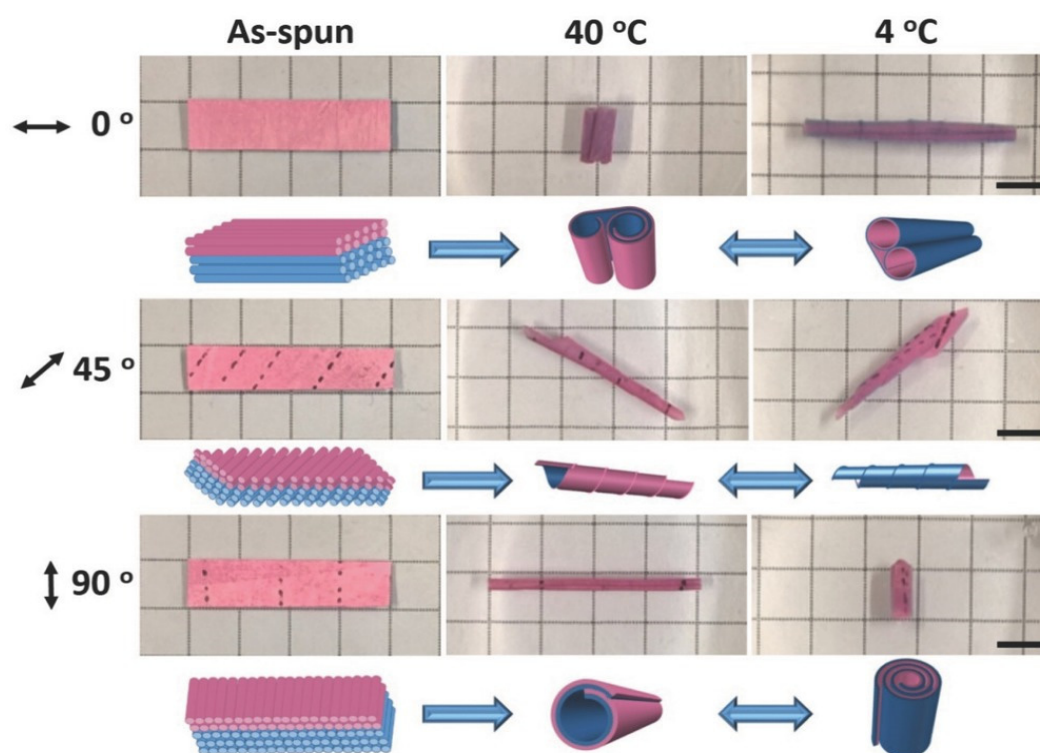


Figure 3. Actuation behavior of fibrous bilayer systems with fiber orientation-dependent shape shifts. Reprinted with permission from [59]. Copyright 2016 John Wiley & Sons, Inc.

Besides heat as stimulus to induce an actuation function, light responsive electrospun hydrogel actuators were reported, which were inspired by the hierarchical structure of a whale baleen [61]. The actuators were designed via *in situ* polymerization of pyrroles on nanofiber-oriented electrospun and temperature-responsive P(NIPAM-ABP) hydrogels. The coating with polypyrroles on nanofibers enhanced mechanical strength (from 1.21 to 5.12 MPa of tensile strength) and enabled ultrahigh-efficiency of photothermal conversion. As result of the porous structure of hydrogel nanofibers (high specific surface area), the speed of the light-responsive actuation could be accelerated. When the ultrathin hydrogel layer ($15 \pm 3 \mu\text{m}$) was bonded to a polyethylene glycol diacrylate-cellulose nanofiber (PEGDA-CNF) composite hydrogel membrane by means of interfacial UV-polymerization, an anisotropic bi-hydrogel actuator was obtained. This actuator showed various programmable complex deformations with a powerful force (can grab up 100 times of self-weight), rapid speed (1285.71 °/s of folding, 32.73 °/s of bending, and 434.36 °/s of bending recovery), and was utilized to

imitate a continuous crawling movement of a starfish (Figure 4). Reversible movements in hydrogel actuators initiated by electric currents were realized in a system based on fibers from acrylic acid (AA), PEG-diacrylate, acrylamide (AAM), and PVA that were *in situ* photopolymerized together with polyaniline formation [62]. The obtained hybrid hydrogel mats showed high electric conductivity. A fast actuation behavior ($2.5 \text{ mm}\cdot\text{s}^{-1}$) could be reached by applying low voltage (1V) and low current ($5 \mu\text{A}$). By coupling a load cell to the electrochemical cell, generated forces could be monitored, which reached about $80 \mu\text{N}$.

It has to be noticed that most of the presented examples showed an actuation behavior based on swelling and deswelling effects which cause a stress mismatch in bilayer systems. While complex shape shifts can be obtained by cutting bilayer systems at different angles or by combining electrospinning and 3D printing, the macroscopic movement is dependent on processing parameters (e.g., alignment of fibers). In contrast to that, SMPs can perform numerous different shape shifts by programming them into versatile temporary shapes (new synthesis is not required), but electrospun hydrogel actuators, which provide shape-memory properties and are swollen during the whole shape-memory cycle were not reported so far. Shape-memory hydrogels often include hydrophobic crystallizable switching segments [63,64]. In contrast to this, electrospun SMPs were reported based on hydrophilic crystallizable switching segments, which demonstrated the recovery to the original shape when a high amount of water was uptaken (crystalline domains were dissolved and a hydrogel was created) [65,66]. Polyurethanes were stretched or folded in the swollen state in water hydrogel actuators, which provide shape-memory properties and are swollen during the whole shape-memory cycle were not reported so far. Shape-memory hydrogels often include hydrophobic crystallizable switching segments [63,64]. In contrast to this, electrospun SMPs were reported based on hydrophilic crystallizable switching segments, which demonstrated the recovery to the original shape when a high amount of water was uptaken (crystalline domains were dissolved and a hydrogel was created) [65,66]. Polyurethanes were stretched or folded in the swollen state in water and in a subsequential drying step, crystallization of PEG enabled the fixation of the temporary shape. Once water was added, a rapid shape recovery to the original shape was achieved at room temperature.

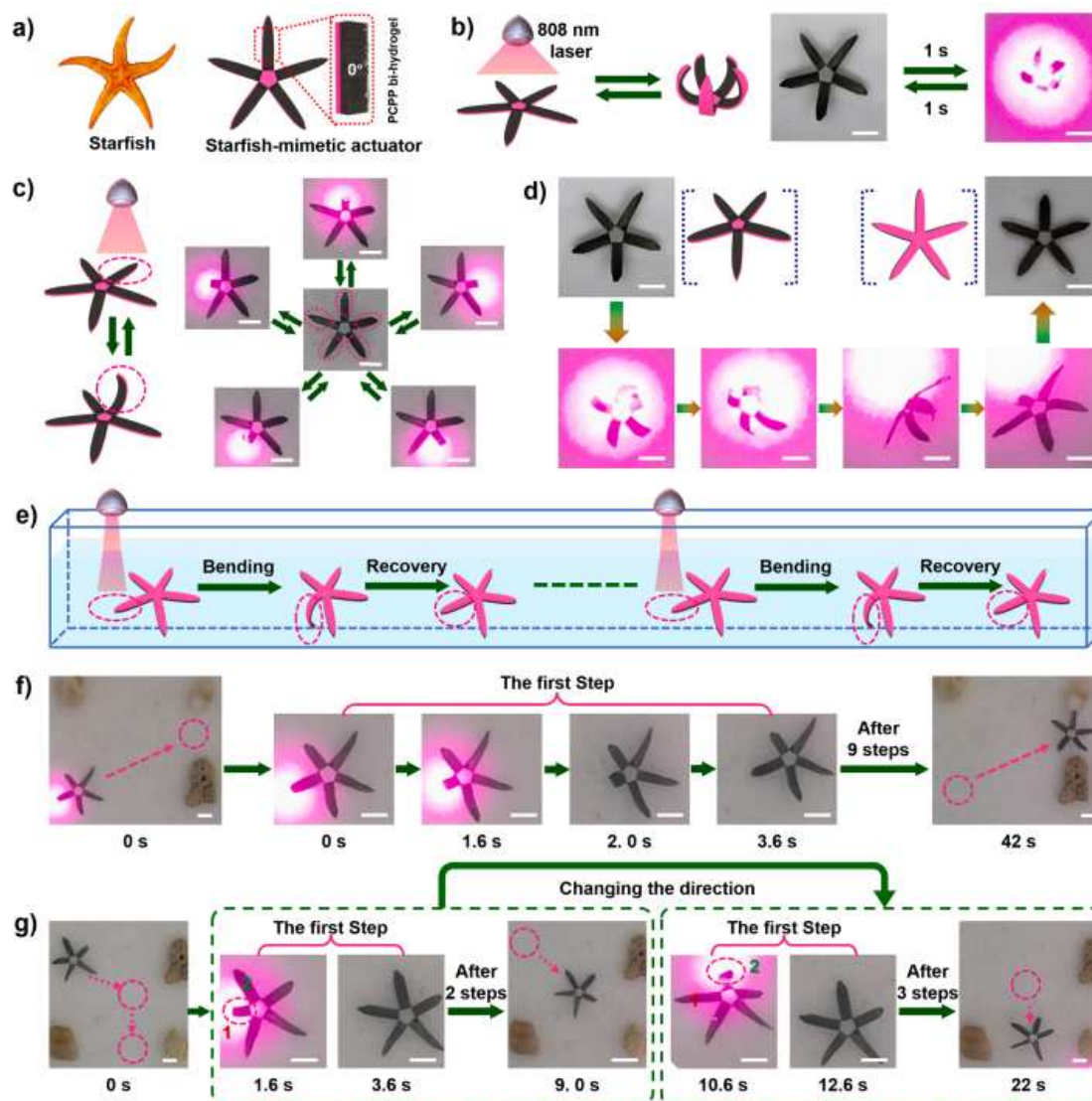


Figure 4. The starfish-mimetic actuating device. (a) The anisotropic structure of the starfish-mimetic actuating device. (b) The synchronized upward bendings of the legs on the starfish. (c) The one-by-one bendings of the starfish legs. (d) The turning-over process of the starfish. (e) Illustration of the continuous crawling movement of the starfish. (f) The continuous forward crawling movement and g) the crawling movement in different directions of the starfish. Reprinted from [61], Copyright 2023, with permission from Elsevier.

3.2. Hydrogel actuators with multi-stimuli response

In order to imitate the motion of soft materials such as living organisms, which act in an environment where multiple stimuli are simultaneously present, hydrogel actuators providing multi-stimuli response were designed. When e.g., a P(NIPAM-ABP) layer and a Fe_3O_4 /polyacrylonitrile (PAN) layer are combined to obtain an anisotropic bi-layer hydrogel actuator, multiple stimuli-responsiveness with programmable bi-functional synergistic movements can be realized [67]. Here, a bilayer structure was developed by electrospinning of a PAN solution doped with Fe_3O_4 nanoparticles and a solution based on precursors for P(NIPAM-ABP). After crosslinking, a composite hydrogel, which was equipped with a thermo-responsive (P(NIPAM-ABP)) and a magneto-responsive layer (Fe_3O_4 /PAN) was obtained. The Fe_3O_4 /PAN layer could perform long-range directional navigation highly controlled by a magnetic field on account of the doping of magnetic nanoparticles. In addition, the efficiency of the Fe_3O_4 nanoparticles endowed the P(NIPAM-ABP)

layer with fast remotely-controlled photothermal-responsive deformations (178°/s) when NIR light was applied. Here, resulting swelling / deswelling effects triggered the macroscopic movements.

Depending on the functional groups in the hydrogel, the swelling behavior could also be dependent on pH. In this case, any pH-responsive group (e.g., acids, amines, or pyridines) in a hydrogel matrix can initiate pH-responsive swelling effects by deprotonation or protonation. As example, thermo- and pH-responsiveness was realized by in electrospun poly(NIPAM-co-AA) fibers, which were embedded within a passive TPU matrix [68]. The resulting composite had a gradient of the TPU along the thickness. At low pH value, the size of the demonstrator was controlled by the temperature (swelling at 6 °C, shrinkage at 40 °C). When the pH-value was changed from pH = 3 to pH = 10, AA moieties were deprotonated and the generated charge repulsion was increasing the swelling. As a result, directed movements were obtained based on generated stresses in the composite and the angle, at which fibers were embedded in the matrix controlled the actuation direction. In addition, thermo- and pH-responsiveness was demonstrated by multi-layer hydrogel actuators, which were fabricated by combining electrospinning and hydrogel lithography [69]. The combination of stimuli-responsive hydrogel fibers based on PAA and/or PNIPAM as active layer(s) with a PCL-based passive layer by a micropatterned hydrogel coupling layer caused the reversible movement of the resulting actuators when the pH or temperature was changed. Here, shape shifts were regulated by modulating the mechanical properties of the actuator materials and dimensions of hydrogel micropatterns. Utilizing the presented actuating system, artificial muscles providing holding, grabbing, transferring, and releasing behaviors as prototypes were fabricated. These examples show that easy incorporation of composite materials or changing the type of active layer enables the design of multi-responsive hydrogels actuators. Hence, prototypes of these multi-stimuli sensitive hydrogel actuators could act in an environment where numerous stimuli are present in a predefined manner.

4. Electrospun shape-memory polymers (SMP) actuators

A number of biological systems exhibit a shape change process when exposed to a wide variety of environmental changes, thus enabling sensing and responsive functionalities [12,70–72]. Synthetic materials can be programmed to intrinsically respond to environmental changes in a similar manner and have the potential to revolutionize material science. One such example is shape-memory polymers, that can recover their original shape after being exposed to an external stimulus, such as heat, light, or a magnetic field [17,22–24]. These materials are unique as they can undergo a transition between a temporary shape and a permanent shape. The polymer is first programmed into a high energy temporary shape by using a specific programming procedure. By exposure to an external stimulus, it reverts to its low energy permanent shape. These polymers have attracted significant attention in recent years due to their potential use in a wide range of applications, including biomedical devices, aerospace, automotive, and textiles [17,22,23,33,63]. Recent studies have focused at the development of shape-memory electrospun fibrous meshes with actuation capabilities. These fibrous meshes have shown interesting advantages over bulk materials such as a faster recovery process, due to the high surface area (in case of a thermally triggered process) and to a faster diffusion (in case of a water triggered process) [73,74]. They have also shown relatively high values of shape fixity and shape recovery ratios, with values ranging between 80% and somewhat higher than 90%. These benefits enable a versatile and customizable platform for developing advanced materials with enhanced mechanical, sensing, and actuation properties for various applications, including biomedical devices, smart textiles, and aerospace components [74]. However, most of these electrospun fibrous meshes are limited to a single, irreversible change in shape or pore size and application of an external stress is required to program the sample [75]. Only few reports deal with reversible actuations or programmable pore size changes under stress-free conditions in electrospun fibrous meshes.

Electrospun SMPs based on covalently crosslinked poly(ϵ -caprolactone) (cPCL) fibrous meshes enabled a bidirectional reversible actuation and a temperature-controlled reversible change in porosity [76]. A two-step preparation procedure was used to achieved cPCL fibrous meshes. In the

first step the electrospinning of a blend of PCL with triallyl isocyanurate (TAI) and benzophenone (BP) was carried out, while in the second step the as spun fiber meshes underwent photo-initiated crosslinking process (Figure 5a,b). To observe the actuation behaviour, the meshes underwent deformation at an elevated temperature and cooling while keeping the deformation strain (Figure 5c). After the programming step, the actuation of the meshes was triggered by heating and cooling between 10 °C and 60 °C as shown in Figure 5d. The actuation performance of the cPCL fibrous meshes was dependent on the programming strain. For a programming strain of 100%, a reversible microscopic reversible actuation strain of $\epsilon'_{rev} = 6\% \pm 1\%$ was measured, while it was increased to $22\% \pm 1\%$ for a programming strain of 300% as shown in Figure 5d. The actuation performance was significantly higher in meshes ($\epsilon'_{rev} = 15\%$) as compared to pure cPCL film with the same strain, and this was attributed to the higher orientation of the molecular chains through the electrospinning process. Furthermore, SEM was carried out to observe a reversible change in the pore sizes at different temperature under stress-free condition. An apparent change of individually measured pore size of $11 \pm 3\%$ during actuation, from an average value of $10.5 \pm 0.5 \mu\text{m}$ at 60 °C to $11.8 \pm 0.6 \mu\text{m}$ at 10 °C was obtained for the cPCL fiber meshes during an in-situ measurement process as shown in the Figure 5e.

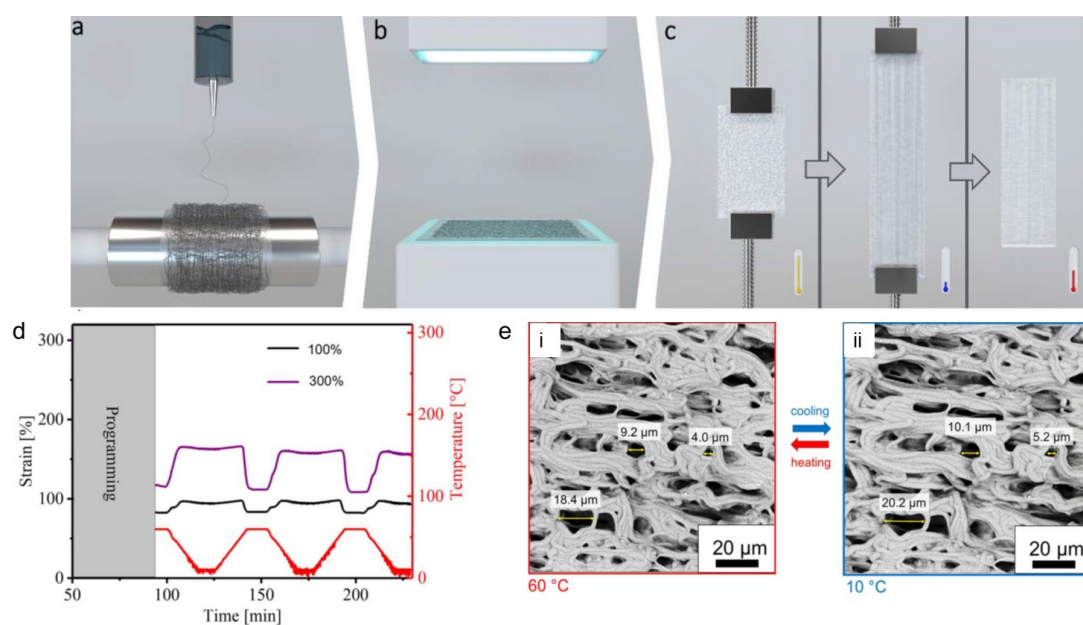


Figure 5. Schematic illustration of the fabrication and programming of electrospun fibers, (a) electrospinning (b) crosslinking (c) programming (d) Cyclic mechanical tensile tests (between 60 °C and 10 °C) of cPCL meshes with strain of 100% (black curve) and 300% (purple curve). The temperature curve is shown in red. (e) SEM image of cPCL heated to 60 °C (i) and after cooling at 10 °C (ii); exemplary pore diameters in the direction of deformation are shown. Reproduced from [76], Copyright 2019, with permission from IOP Publishing Ltd.

To see the effect of different spatial arrangements of stacked fiber bundles on the actuation behaviour, electrospun fiber meshes based on poly(ethylene-co-vinyl acetate) (PEVA) with different crosslinking densities were fabricated [77]. UV-based crosslinking was conducted to affect the interfiber bond strength by using TAI as a crosslinker and BP initiator. The SEM images of fiber mesh actuators with different fiber alignments (random, aligned, stacked 0-90 °) are shown in Figure 6a. To prove an inter-fiber or intra-fiber crosslinking, the tensile testing of the aligned PEVA fibers in the crosslinked or uncrosslinked state along the fiber direction ($\delta = 0^\circ$ to observe the intra-fiber bulk properties), and perpendicular to the fiber ($\delta = 90^\circ$ to evaluate the inter-fiber bonds) was carried out. The crosslinking resulted in an increase in peak stress and decrease in elongation at break for both cases indicating the presence of both inter-fiber and intra-fiber crosslinking (Figure 6b,c).

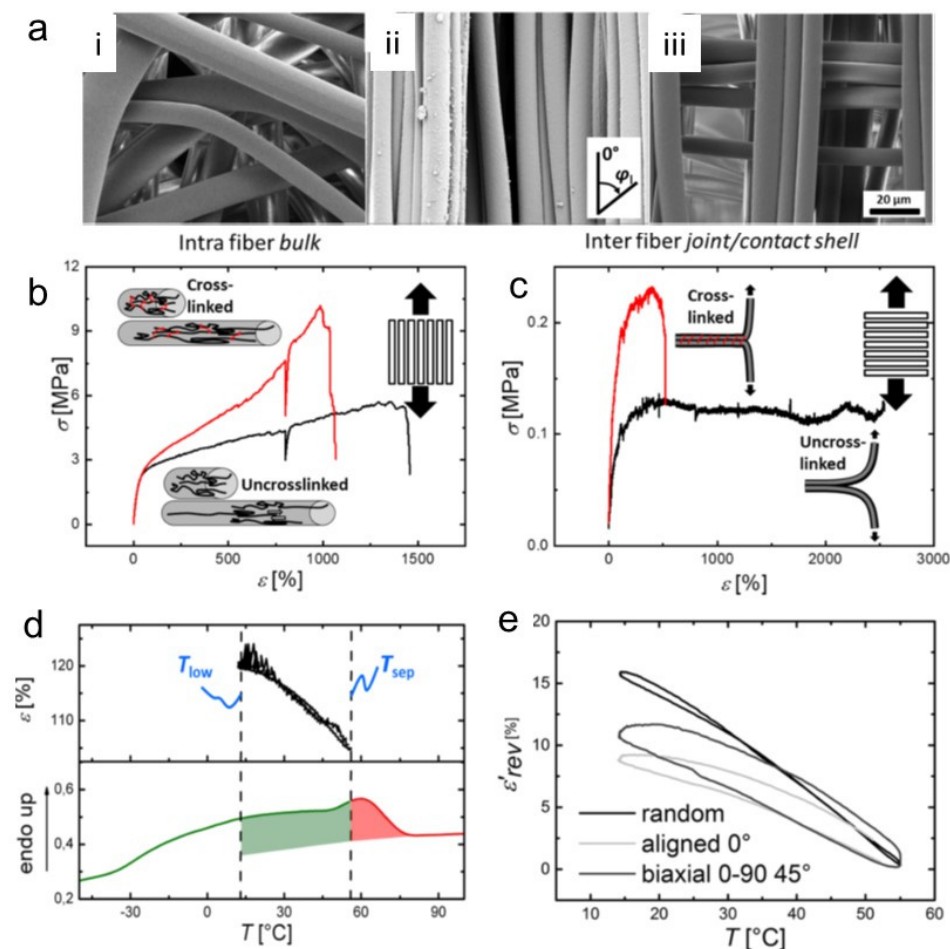


Figure 6. (a) SEM images of PEVA fiber meshes after electrospinning process at RT with different fiber arrangement. (i) random, (ii) aligned, (iii) stacked 0-90. (b,c) Mechanical properties of aligned fiber bundles at RT of the crosslinked (red curves) and uncrosslinked (black curves) fibers as well as a schematic description of the molecular processes at different strains. The red color utilized in the schemes denotes covalent crosslinks. (b) Loading along the fiber direction; (c) Perpendicular to the fiber direction. (d) Actuator capability after implementing by thermomechanical programming procedure. *Upper:* Reversible elongation and contraction by cooling and heating between T_{low} and T_{high} . *Lower:* DSC curve showing the broad thermal transition of the crosslinked electrospun fiber mesh scaffold. The curve is separated $T_{sep} = 55$ °C into a green and red color. Green: melting temperature range related to actuation units; Red: melting temperature range related to geometry determining units. (e) Reversible actuation strain ϵ'_{rev} depending on different fiber alignment after the samples have been programmed. The original data points were smoothed by adjacent averaging. Random: black curve; Biaxial (0-90) (45°): grey curve; Aligned 0°: light grey curve. Reproduced from reference [77], Copyright 2022, with permission from Elsevier.

The actuation performance found in all fiber mesh geometries comprised a ϵ'_{rev} of $17 \pm 2\%$ for random, $10 \pm 1\%$ for aligned fibers along the fiber ($\delta = 0^\circ$) and $12 \pm 1\%$ for 0-90 biaxial meshes in $\delta = 45^\circ$. The improved actuation capability in random meshes was attributed to an increased shape deformation in the initial heating to T_{sep} from the temporary shape $\epsilon_u = 148\%$ to $\epsilon_{T,sep}$ around 105%, while ϵ'_{rev} varies below and above the programming strain $\epsilon_{ssp} = 150\%$ for aligned fiber meshes ($\epsilon_u = 150\%$, $\epsilon_{T,sep} = 144\%$). The stronger initial shape deformation of the random mesh could be related to a microstructural as well as molecular aspect (Figure 6d,e).

To avoid the secondary crosslinking step by exposure to UV light, in situ crosslinking of electrospun fibers based on stereocomplexation was studied. Blending of a multi-block copolymer containing poly(L-lactide) and poly(ϵ -caprolactone) segments (PLLA-PCL) with oligo(D-lactide)

(ODLA) in a one-step solution-casting process resulted the formation of a stereocomplex [78]. This physical networking between the opposite enantiomers of PLA organized them into a periodic crystalline structure. The actuation behavior of the electrospun meshes and the bulk material was tested. The electrospinning process resulted a higher molecular orientation enabling an improved shape-memory actuation performance in microfiber meshes compared to the bulk material. The actuation magnitude of $\epsilon_{rev} = 5.5 \pm 0.5\%$ in bulk PLLA-PCL/ODLA blends was increased to $7.8 \pm 0.8\%$ in fibrous meshes. Twisting the electrospun fibers into a yarn, resulted a further increase of actuation to $15 \pm 1.8\%$. This was attributed to the improvement of the structural integrity of the fibers. The simultaneous orientating of polymer molecules and their cross-linking into a physical network, opens a broad perspective for the development of actuating fiber meshes.

5. Electrospun electroactive actuators

Electrochemical devices such as actuators can work due to conversion of chemical reactions into electrical energy. Due to the high surface to volume ratio of nanofibers and the porous structure of nanofibrous meshes, electrospun nanofibers have led to the fabrication of high-performance and versatile electrochemical devices [79–81]. One of the most promising application of such devices are artificial muscles, which can mimic the function of natural skeletal muscles, and therefore, have potential applications in biomimetic robots and biomedical devices [5,7]. In recent years, various nanomaterials have been utilized to obtain artificial muscles and improve their mechanical, electrical, and electrochemical properties [82,83].

Actuation of such devices can happen according to two mechanisms based on electromechanical and electrochemical reactions. Electromechanical (electric) actuation is related to electric dipole rearrangements in electroactive polymers that cause dimensional changes, while electrochemical mechanisms utilize electrostatic forces, in which the ion exchange mechanism is responsible for volume changes in ionic electroactive polymers (EAP) [84,85]. In comparison to electronic EAP, ionic EAP offers significantly lower voltage (1-2 mV), therefore, they can find application in medical field, especially in preparation of artificial muscles. Furthermore, in case of ionic EAP dimensional changes remain stable even after cutting off the electrical potential. To return to initial dimensions the reverse potential is required. Furthermore, the wireless electrochemical actuation of ionic EAP-based artificial muscles has been investigated, which could eliminate the need of a direct physical connection to an electric power supply [15,86].

Much attention has been paid to the fabrication of conductive polymer-based actuators having nanofibrous structures [87,88]. However, direct fabrication of conducting polymer nanofibers using the electrospinning process is challenging due to the fact that typically polymers with low molar mass are produced that show inherent brittleness, as often the corresponding monomers have poor solubility in common solvents [89]. Therefore, several alternative approaches have been utilized to incorporate conducting polymers (CPs) into fibrous structures. The most common are: co-axial electrospinning to produce core-shell nanofibers and preparation of electrospinnable blends of polymers with CPs, which can be processed by electrospinning [90–92]. However, they result in a formation of nanofibrous layer with low electrical conductivity and poor electrochemical properties for use as an actuator. A direct polymerization of CPs on the surface of the substrate nanofibers is a simple and versatile technique for producing CP nanofibers of a core-shell structure [93]. There, a conducting polymer layer is on the surface of the fibers, which provides an effective nanofibrous conducting polymer-based actuator [94]. Furthermore, it was found that a multilayered cylindrical structure of the nanofibrous mesh increases the active surface area of the actuator and thus facilitates the diffusion of the ions [95].

For the purpose of electrospun electroactive actuators, biopolymers such as cellulose [96,97], cellulose acetate (CA) [27], gelatin [98], chitosan [99–101], and silk [102] have been considered, particularly in biological and medical applications [79]. In most of the cases, the biopolymer-based nanofibrous substrate is intended to increase biocompatibility of the actuator. However, some biopolymers, such as CA, have naturally electrical actuation ability, which, due to the synergistic effect with the active component, improves the final actuation performance of the bioactuators

[16,103]. Furthermore, due to the doping ability, CPs such as polypyrrole (PPy) [104,105], poly(3,4-ethylenedioxythiophene) (PEDOT) [94], or polyaniline (PANI) [98,106] could be used in conjunction with biopolymers to produce fibrous bioactuators for in vitro or in vivo applications [32,107].

CPs are good candidates for manufacturing devices that mimic natural muscles due to their chemical structure, which expands and contracts due to a flux of ions/solvent in and out of the polymer matrix when the conjugated backbone is electrochemically oxidized and reduced when low voltages are applied (1–2 V) in the presence of an electrolyte [108,109]. Beregoi et al. reported metalized PMMA fibers with good transparency, which were applied as working electrode for PANI shell deposition by electrochemical polymerization. By controlling the potential applied, the oxidation state, as well as the color of PANI was easily changed in the presence of an electrolyte. Moreover, the biological investigations revealed a good compatibility with eukaryotic cells for all PANI-coated samples [110]. Also, preparation and actuation ability of PANI/Au microtubes was reported. It was found that such aligned PANI coated microtubes with the inner diameter in the range of microns presented a muscle like behavior, expanding and contracting by switching the potential between -0.2 and 1 V. The bending took place with a response time lower than 10 s [111]. Gu et al. reported a biomimetic myofibril that was made from parallel oriented high-strength polyurethane (PU) and then chemically polymerized with aniline [112]. The electrochemical actuation profile of the PU/PANi nanofibrous bundles is presented in Figure 7a. The PU/PANi hybrid nanofibrous bundle responded to the electrical stimulus resulting in an initial linear strain of 1.6% at an applied stress of 1.03 MPa. Those artificial muscle fiber bundles have shown 2% of the actuation strain in over 100 cycles with the working efficiency of each cycle higher than 75% (Figure 7b). The PU/PANi nanofibrous bundle shows minor creep up to 11 mN load (2.3 MPa), above which it shows significant creep behavior in actuation. Furthermore, by incorporation of graphene the actuation performance of this nanofiber slightly decreased, but its modulus is significantly increased [112]. Fengel et al. reported three-layer devices composed of two silk/PPy composite layers separated by an insulating silk layer. The proposed design allowed one side to expand while the other contracts, resulting in improved performance over bilayer actuator making it more symmetric than bilayer analogs and allowing fully reversible operation. As a result, 75% of fabricated devices successfully demonstrated actuation [113]. Hong et al. showed that PANI nanoparticles enhanced the actuation capacity of CA in an electrospun CA/PANI biocomposite film [27]. The harmonic responses for three electrospun actuators responding to sinusoidal electrical inputs with excitation frequency of 0.1 Hz and the voltage amplitude of 3.0 V were measured (Figure 7c,d). The tip displacement of the 0.5 wt% PANI/CA bio-composite actuator was four times larger than in the case of the pure CA actuator, as shown in Figure 7c. Also, the increase of addition of PANI from 0.1wt% to 0.5 wt% improved tip displacement at all tested frequencies. This phenomenon can be explained by the combination of orientation of permanent dipoles under applied electric current and polarization due to displacement of ions and charge injection from electrodes [27].

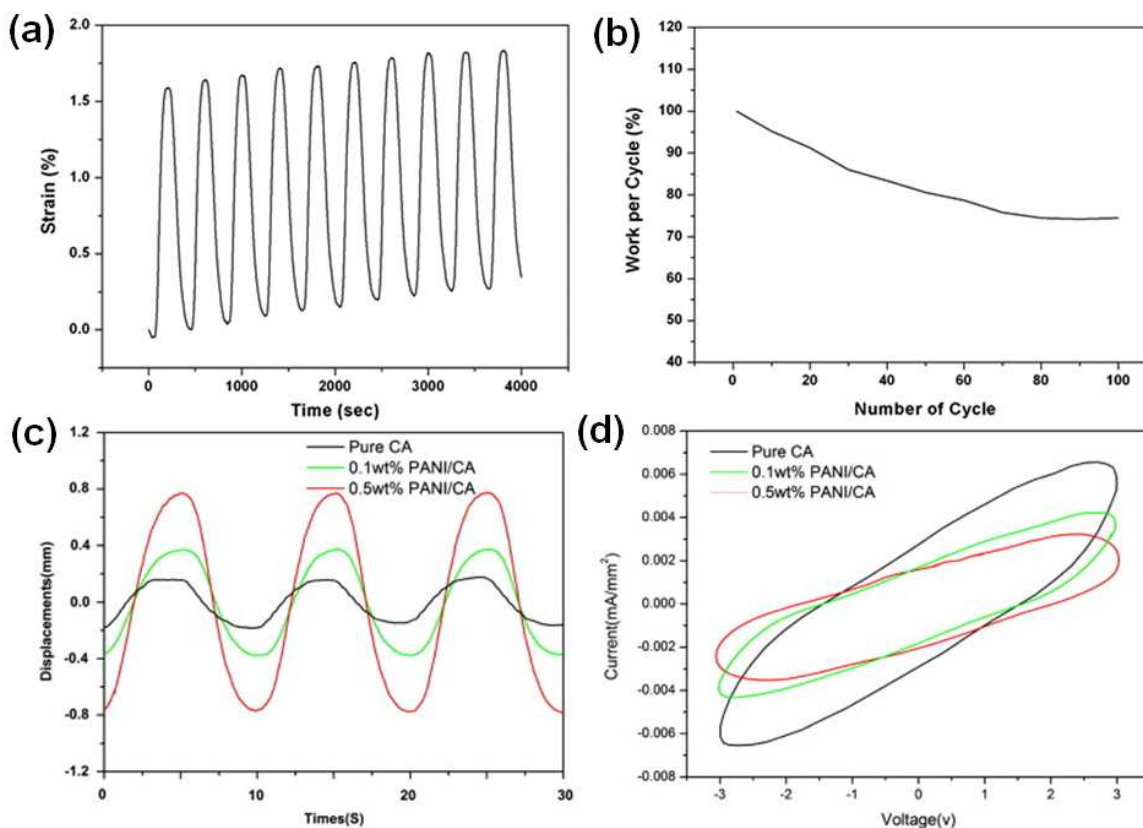


Figure 7. (a) Electrochemical actuation profile of the PU/PANi nanofibrous bundle upon cycling the potential between -0.2 to 0.8 V in aqueous solution of 1 M MSA (scan rate = 5 mV/s, stress = 1.028 MPa) [112]. (b) Work per cycle relating to the stability of PU/PANi hybrid nanofibrous bundle (Electrolyte = 1 M MSA, scan rate = 5 mV/s, potential vs Ag/AgCl) [112]. Reproduced with permission from [112], Copyright 2009 with permission from American Chemical Society. (c) Harmonic responses of the electrospun PANI/CA actuators powered by sinusoidal electrical inputs with excitation frequency of 0.1 Hz and peak voltage of 3 V; time history of tip displacements [27], (d) Hysteresis responses of current–voltage plots for PANI/CA actuators. Reproduced from [27] with permission from Elsevier, Copyright 2013.

An electroactive polymer actuator composed of poly(vinylidene fluoride) (PVDF) membranes enhanced with bacterial cellulose nanowhiskers (BCNW) was developed using electrospinning [114]. The actuating performance was reported as ± 3.4 mm and 4.5 mm for the sinusoidal and step inputs.

PPy has been frequently used to develop soft artificial muscles [115]. Beregoi et al. have reported PPy actuator based on Nylon 66 electrospun microribbons. The microribbons were one side coated with a gold layer, and finally a conductive layer of PPy was added by means of electrochemical deposition [116]. The electroactive microribbons expand and shrink by switching the applied current or potential. The conformational changes of the polymer chains was due to the insertion/expulsion of the ions from the electrolyte (NaCl) and electrons from gold. Furthermore, the asymmetry and anisotropy of the PPy-covered microribbons leads to irregular volume changes, inducing the straightening/twisting of the entire piece. Furthermore, these electrospun actuators were able to show a simultaneous actuation and sensitivity, which is essential for the complex activity of artificial muscles [13]. Bunea et al. presented a new architecture of an artificial muscle based on a gold covered Nylon 66 microfiber electrode attached to a thin foil of PDMS. The PDMS-based artificial muscle showed excellent stability in 500 cycles test while applying a voltage of 2.2 V (Figure 8) [117].

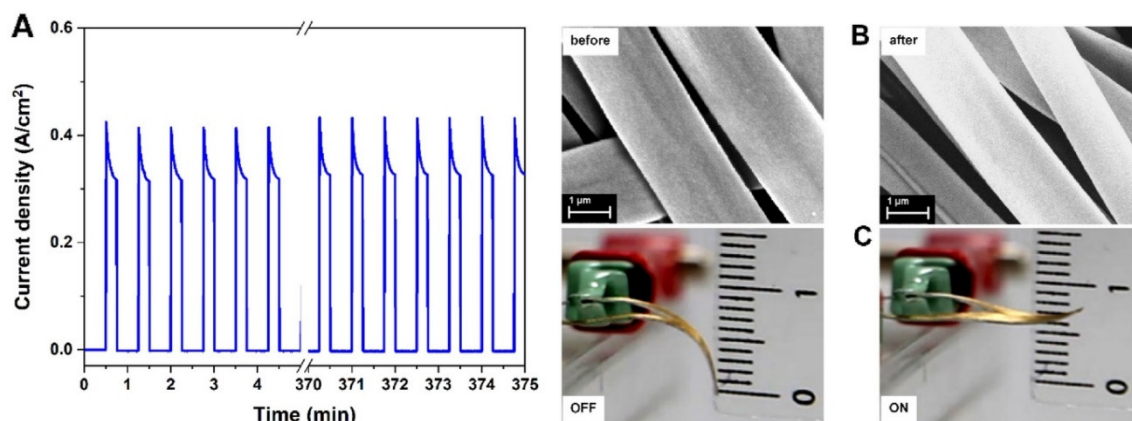


Figure 8. Artificial muscle life time. (A) The current density registered for 500 actuation cycles; (B) SEM images of the metalized electrospun fiber network attached on PDMS sheet before and after 500 ON/OFF voltage cycles; (C) Snapshots taken after 500 actuation cycles of the artificial muscle. Reprinted with permission from [117], Copyright 2022.

Severt et al. synthesized aligned silk/PPy nanofibrous bundles using electrospinning and sequential chemical and electrochemical polymerization processes [36,112]. In the same study, also poly(hydroxymethyl-3,4-ethylenedioxythiophene) (PEDOT-OH) was electrochemically polymerized on the surface of silk nanofibers. Samples were doped with *para*-toluene sulfonic acid (*p*-TSA) or sodium dodecylbenzenesulfonate. The results revealed that the actuation stress and response time of the silk/PEDOT-OH nanofibrous actuator are better than those of the silk/PPy sample. Devices doped with *p*-TSA exchanged both anions and cations, with anion exchange being the dominant mechanism. Furthermore, core-shell nanofibers were prepared by gas-phase polymerization of PEDOT on the surface of PU electrospun fibers and were found to increase the distance actuated by CP actuators, whereas addition of the graphene nanoplatelets to PU-PEDOT nanofiber mats reduced actuator displacement because of a high modulus [118].

Recently, Harjo et al. coated PPy on the surface of glucose-gelatin nanofibers to prepare a linear bioactuator [119]. It should be underlined that PPy coated the glucose-gelatin nanofibers individually, not as a bulk phase. The nanofiber material exhibited electro-chemo-mechanical activity in both aqueous and organic (PC) electrolyte solutions, with good conductivity ($0.45 \text{ S}\cdot\text{cm}^{-1}$) as well as actuation strain (1.2%) and stress (3.15 kPa) values. Furthermore, 120 cycles of strain/stress change revealed no significant loss of strain or stress. Beregoi et al. evaluated the actuators based on PPy-coated metalized eggshell membranes. Electrochemical actuation in a potential cycle between 0.6 and +0.6 V showed that PPy oxidation and reduction result in the insertion and expulsion of electrolyte ions and solvent molecules into and out of the structure resulting in mechanical movements.

Furthermore, upon various conditions of the humidity, actuators were able to move, hold, and release delicate and lightweight objects [120]. Another PU/PPy nanofiber actuator was prepared by Ebadi et al. During the cyclic voltammetry responses PU/PPy actuators consumed total charges of 2.0–5.0 C in the 0.1 M LiClO₄ electrolyte solution in potentials ranging between -0.6 and 0.8 V [26]. The mechanism of the actuation process explained by authors is shown schematically in the Figure 9. During the oxidation process the electrons are extracted from PPy, whereas in the reduction process electrons are injected into it. Therefore, the perchlorate anions and water molecules enter the polymer structure from the electrolyte solution during the oxidation process of the actuators and they leave the polymer structure during the reduction process to balance the electric charge and osmotic pressure. This phenomenon results in a change in the volume, and therefore in the bending angle of produced actuator due to the mechanical constraint imposed by the inactive adhesive tape (Figure 9) [26].

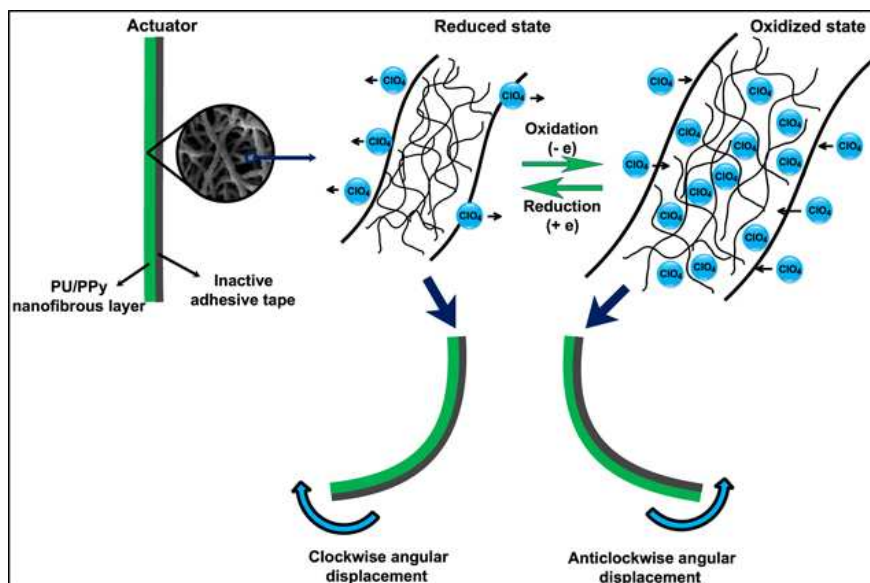


Figure 9. The schematic representation of bending actuation mechanism of the PU/PPy nanofibrous actuators during oxidation and reduction processes. Reprinted with permission from [26], Copyright 2020, with permission from IOP Publishing Ltd.

Gotti et al. prepared PU/PPy-based hierarchically arranged nanofibrous structures similar in architecture and passive mechanical properties to skeletal muscles. The structure of obtained electrospun membrane was packed in a form of bundles taugt together as the biologic membrane epimysium does in the skeletal muscle (Figure 10) [121].

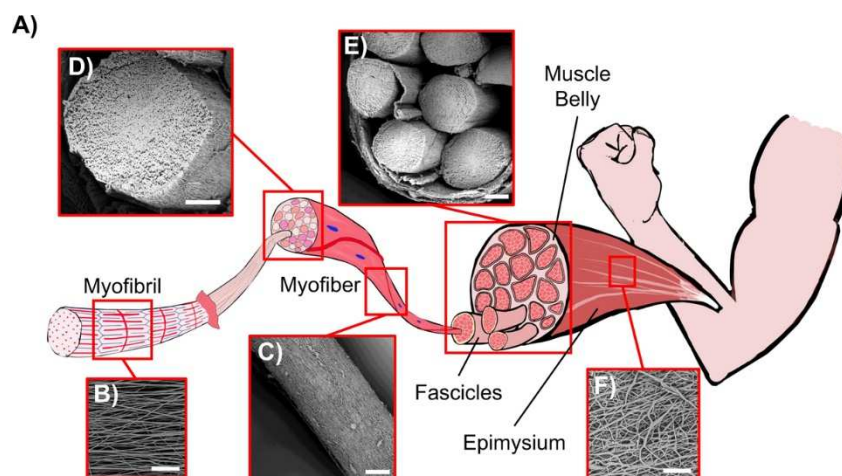


Figure 10. Comparison between the biological skeletal muscle and the electrospun PU structures. (A) Schematics of the hierarchical structure of the skeletal muscle. (B) Mat of aligned nanofibers. The single nanofiber corresponds to a myofibril (scale bar = 20 μm); (C) Bundle of aligned fibers, corresponding to a myofiber (scale bar = 100 μm); (D) Cross-section of an aligned bundle, showing the parallel arrangement of the inner nanofibers (scale bar = 100 μm). (E) Cross-section of the hierarchical nanofibrous electrospun structure (HNES), compared to the cross-section of a biological muscle belly (scale bar = 150 μm); (F) HNES membrane, resembling the epimysium membrane that envelops the muscle belly (scale bar = 100 μm). Reprinted with permission from [121], Copyright 2020, with permission from Frontiers.

6. Electrospun actuators based on liquid crystal elastomers (LCE)

LCE constitute a class of materials, which possess both elastic properties as conventional elastomers and anisotropic physical properties due to the liquid crystalline state of order. LCE-based

microfiber actuators based on nematic-isotropic phase transition of liquid crystal mesogens were reported to generate large actuation strain of 60% with simultaneous fast response <0.2 s and a high power density of 400 W/kg. Furthermore, when coated with a polydopamine layer, the actuation of the electrospun LCE microfiber could be precisely and remotely controlled by a near-IR laser through photothermal effect. As a result, He et al. were able to successfully construct a microtweezer, a microrobot, and a light-powered microfluidic pump using the electrospun LCE microfiber actuator (Figure 11) [122]. Krause et al. obtained electrospun crosslinked nematic fibers with an uniform alignment [19]. These highly oriented fibers exhibited a liquid crystalline state at ambient conditions.

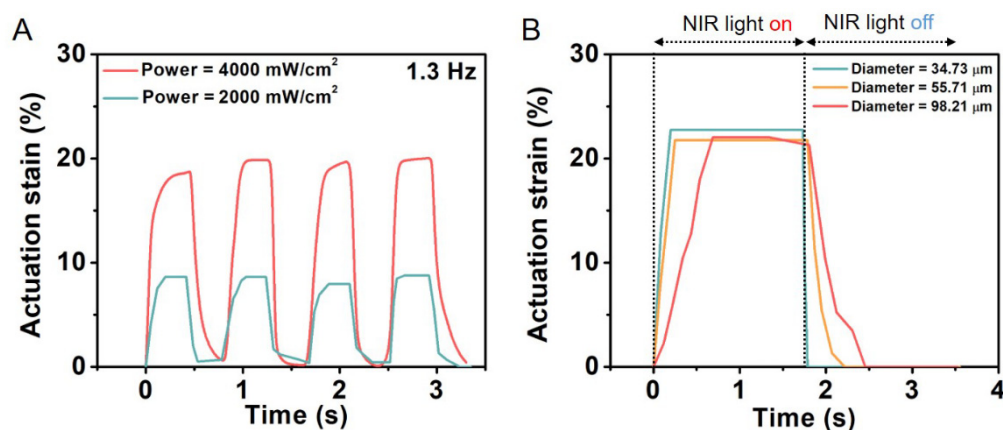


Figure 11. The response of PDA-coated LCE microfibers with different diameters exposed to Near-IR light of two different powers. From Supplementary Materials of [122]. Reprinted with permission from AAAS.

7. Summary and outlook

Electrospinning has emerged as a modern and versatile fabrication technique, offering unique advantages for the production of advanced materials with diverse applications. This review highlights the fascinating field of bioinspired electrospun polymer actuators, focusing on three major categories: stimuli-sensitive hydrogels, shape-memory polymers (SMP), and electroactive polymers [1]. These advanced materials hold tremendous promise in various applications, ranging from soft robotics and biomedical devices to energy harvesting and artificial muscles [7].

Through the ingenious combination of electrospinning and hydrogel technology, intricate fibrous structures are crafted, resulting in actuators that exhibit remarkable shape-changing abilities in response to external stimuli. Despite the promising capabilities of electrospun actuators based on hydrogels, several challenges loom ahead. For instance, selecting hydrogel materials that can be effectively electrospun, while retaining their responsive properties is a complex task, as not all hydrogels can withstand the electrospinning process. Hydrogels are known for their soft nature, creating electrospun actuators that exhibit both responsive behavior and mechanical robustness is intricate [123]. The hydrogel actuators are often based on bilayer structures, in which a swelling / deswelling effect in the active layer generates an internal mechanical stress resulting in a bending movement of the actuator material. In this case, complex shape shifts can only be addressed by different fiber orientations or subsequential 3D printing on electrospun membranes. When another kind of movement is mandatory, new material design is required. Electrospun hydrogel actuator with shape-memory capability are not realized so far. Here, the challenge would be the combination of stimuli-sensitive domains with swelling domains, in which the two different types should act independent from each other (swelling should not influence the stimuli-sensitive domain; stimulus should not influence the swelling domains). Overall, the incorporation of additional functionalities, such as, sensing or controlled drug release, while maintaining the actuator's responsive behavior requires careful material selection and design.

SMP fibrous meshes have shown immense potential and exciting prospects for the cutting-edge technology in the field of soft robotics and beyond [73]. However, achieving reproducibility and scalability remains a challenge. The process can be intricate and sensitive to parameters, leading to inconsistencies in fiber morphology, size, and distribution. Ensuring robust mechanical properties of electrospun SMPs while maintaining their shape memory behavior is a delicate balance. Achieving high mechanical strength and elastic modulus without sacrificing actuation performance is an ongoing challenge. The characterization of electrospun SMPs, particularly at the nano-scale, demands sophisticated and precise techniques. Developing non-destructive, high-resolution methods to study structure-property relationships is crucial. Addressing these challenges will require concerted efforts from researchers, engineers, and industry stakeholders to unlock the full potential of electrospun SMPs and transform them into practical and impactful materials for a wide array of applications.

Electrospun actuators harnessed from conductive polymers (CPs) leverage the unique electroactive properties of polymers, responding to electrical stimuli with dynamic shape changes. However, due to poor physical features induced by insolubility, infusibility, and brittleness, applicability of CPs as actuators requires significant challenges to be addressed. As the utilization of electrospinning requires organic solvents for the preparation of solution, therefore, synthesis of new CPs by modification of existing CPS or synthesis of new derivatives with improved solubility and spinnability are mandatory. Furthermore, finding or synthesizing better organic solvents or functional doping agents would be a promising direction, which is critical for realistic applications. Nevertheless, there is severe concern for the application of electrospun CPs in the medical field, as for example biosensors, bio-actuators, and tissue engineering scaffolds due to the risk of cytotoxicity caused by residual solvent and solvent accumulation. Due to this reason, the use of melt-electrospinning to produce fibers with reproducible diameter and structure of electrospun 3D materials, seems to be perspective [81,101,124]. However, CPs are difficult to melt into electrospun fibers, which opens new ways for post-treatments or combined methods of fiber preparation.

Considering the present state of art, a great challenge is to reach a large-scale production of electrospun fibers and 3D materials and their commercialized applications. Electrospinning process is still mostly investigated in academic laboratories with the usage of single-needle electrospinning device. Therefore, more attention should be paid to the development of this technique, which would enable various multi-needle/multi-jet electrospinning and nozzle-less electrospinning techniques [125,126]. Furthermore, the potential of hybrid materials that combine stimuli-sensitive hydrogels, shape-memory polymers, and electroactive polymers is particularly emphasized, as such combinations may unlock unprecedented actuation capabilities and multifunctionality. Moreover, the integration of emerging technologies like nanotechnology and additive manufacturing could further enhance the performance and efficiency of these actuators. In the biomedical field, the development of biocompatible and bioresorbable materials opens up exciting possibilities for implantable devices and tissue engineering applications. Collaboration between different disciplines, such as materials science, engineering, and biology, will be crucial in overcoming challenges and accelerating the translation of these bioinspired actuators from the laboratory to real-world applications. In conclusion, this review paper serves as a comprehensive resource for researchers and enthusiasts interested in the cutting-edge developments of bioinspired electrospun polymer actuators. By fostering collaboration and innovation, this field holds the potential to revolutionize numerous industries and bring us closer to achieving highly adaptable, bioinspired systems with a wide array of practical applications.

Author Contributions: Conceptualization, M.Y.R. and M.B.; methodology, M.M.; software, M.Y.R. and M.M.; validation, M.Y.R., M.B. and M.M.; formal analysis, M.Y.R.; investigation, M.B.; resources, M.M.; data curation, M.B.; writing—original draft preparation, M.Y.R., M.B. and M.M.; writing—review and editing, M.B.; visualization, M.Y.R.; supervision, A.S.; project administration, M.B.; funding acquisition, M.B. and M.M. All authors have read and agreed to the published version of the manuscript.

Funding: This work is supported by the Helmholtz Association through program-oriented funding and received funding from the European Union's Horizon 2020 research and innovation program under Grant Agreement No. 824074 (GrowBot). This work was also co-financed by the Department of Chemistry of Warsaw University of Technology under the Project No. 504/04365/1020/44.000000.

Data Availability Statement: Date is contained within the article.

Acknowledgements: The authors acknowledge Axel T. Neffe and Harald Rupp for suggestions for improvement and proof reading.

Conflicts of Interest: The authors declare no conflict of interest.

References

1. S. Poppinga *et al.*, "Toward a New Generation of Smart Biomimetic Actuators for Architecture," *Adv. Mater.*, vol. 30, no. 19, p. 1703653, May 2018.
2. W. Li *et al.*, "An on-demand plant-based actuator created using conformable electrodes," *Nat. Electron.*, vol. 4, no. 2, pp. 134–142, 2021.
3. S. Li and K. W. Wang, "Plant-inspired adaptive structures and materials for morphing and actuation: a review," *Bioinspir. Biomim.*, vol. 12, no. 1, p. 11001, 2017.
4. Y. Chen *et al.*, "Light-driven bimorph soft actuators: design, fabrication, and properties," *Mater. Horizons*, vol. 8, no. 3, pp. 728–757, 2021.
5. Y. Yang, Y. Wu, C. Li, X. Yang, and W. Chen, "Flexible Actuators for Soft Robotics," *Adv. Intell. Syst.*, vol. 2, no. 1, p. 1900077, 2020.
6. Z. Xu, Y. Zhou, B. Zhang, C. Zhang, J. Wang, and Z. Wang, "Recent Progress on Plant-Inspired Soft Robotics with Hydrogel Building Blocks: Fabrication, Actuation and Application," *Micromachines*, vol. 12, no. 6, p. 608, May 2021.
7. T. Mirfakhrai, J. D. W. Madden, and R. H. Baughman, "Polymer artificial muscles," *Mater. today*, vol. 10, no. 4, pp. 30–38, 2007.
8. W. Wang, C. Li, M. Cho, and S.-H. Ahn, "Soft Tendril-Inspired Grippers: Shape Morphing of Programmable Polymer–Paper Bilayer Composites," *ACS Appl. Mater. Interfaces*, vol. 10, no. 12, pp. 10419–10427, Mar. 2018.
9. M. I. Osotsi, W. Zhang, I. Zada, J. Gu, Q. Liu, and D. Zhang, "Butterfly wing architectures inspire sensor and energy applications," *Natl. Sci. Rev.*, vol. 8, no. 3, p. nwa107, Mar. 2021.
10. N. F. Lepora, P. Verschure, and T. J. Prescott, "The state of the art in biomimetics," *Bioinspir. Biomim.*, vol. 8, no. 1, p. 13001, 2013.
11. Y. Dong *et al.*, "Multi-stimuli-responsive programmable biomimetic actuator," *Nat. Commun.*, vol. 10, no. 1, p. 4087, 2019.
12. H. Liu *et al.*, "Bioinspired gradient structured soft actuators: From fabrication to application," *Chem. Eng. J.*, vol. 461, p. 141966, Apr. 2023.
13. M. Beregoi, S. Beaumont, A. Evangelidis, T. F. Otero, and I. Enculescu, "Bioinspired polypyrrole based fibrillary artificial muscle with actuation and intrinsic sensing capabilities," *Sci. Rep.*, vol. 12, no. 1, p. 15019, 2022.
14. H. Cui, Q. Zhao, L. Zhang, and X. Du, "Intelligent Polymer-Based Bioinspired Actuators: From Monofunction to Multifunction," *Adv. Intell. Syst.*, vol. 2, no. 11, p. 2000138, 2020.
15. F. Carpi, R. Kornbluh, P. Sommer-Larsen, and G. Alici, "Electroactive polymer actuators as artificial muscles: are they ready for bioinspired applications?," *Bioinspir. Biomim.*, vol. 6, no. 4, p. 45006, 2011.
16. M. A. Marsudi *et al.*, "Conductive Polymeric-Based Electroactive Scaffolds for Tissue Engineering Applications: Current Progress and Challenges from Biomaterials and Manufacturing Perspectives," *International Journal of Molecular Sciences*, vol. 22, no. 21, 2021.
17. M. Y. Razzaq, J. Gonzalez-Gutierrez, G. Mertz, D. Ruch, D. F. Schmidt, and S. Westermann, "4D Printing of Multicomponent Shape-Memory Polymer Formulations," *Appl. Sci.*, vol. 12, p. 7880, 2022.
18. D. H. Gracias, "Stimuli responsive self-folding using thin polymer films," *Curr. Opin. Chem. Eng.*, vol. 2, no. 1, pp. 112–119, 2013.
19. S. Krause, R. Dersch, J. H. Wendorff, and H. Finkelmann, "Photocrosslinkable Liquid Crystal Main-Chain Polymers: Thin Films and Electrospinning," *Macromol. Rapid Commun.*, vol. 28, no. 21, pp. 2062–2068, 2007.

20. Q. Mu *et al.*, "Robust Multiscale-Oriented Thermoresponsive Fibrous Hydrogels with Rapid Self-Recovery and Ultrafast Response Underwater," *ACS Appl. Mater. Interfaces*, vol. 12, no. 29, pp. 33152–33162, Jul. 2020.
21. S. Agarwal, S. Jiang, and Y. Chen, "Progress in the Field of Water- and/or Temperature-Triggered Polymer Actuators," *Macromol. Mater. Eng.*, vol. 304, no. 2, p. 1800548, Feb. 2019.
22. A. Lendlein and S. Kelch, "Shape-memory polymers," *Angew. Chem. Int. Ed.*, vol. 41, pp. 2034–2057, 2002.
23. P. T. Mather, X. Luo, and I. A. Rousseau, "Shape Memory Polymer Research," *Annu. Rev. Mater. Res.*, vol. 39, no. 1, pp. 445–471, Aug. 2009.
24. M. Behl, M. Y. Razzaq, and A. Lendlein, "Multifunctional Shape-Memory Polymers," *Adv. Mater.*, vol. 22, no. 31, pp. 3388–3410, Jun. 2010.
25. F. F. Li, Y. J. Liu, and J. S. Leng, "Progress of Shape Memory Polymers and Their Composites in Aerospace Applications," *Yuhang Xuebao/Journal of Astronautics*. 2020.
26. S. V. Ebadi, H. Fashandi, D. Semnani, B. Rezaei, and A. Fakhrali, "Electroactive actuator based on polyurethane nanofibers coated with polypyrrole through electrochemical polymerization: a competent method for developing artificial muscles," *Smart Mater. Struct.*, vol. 29, no. 4, p. 45008, 2020.
27. C.-H. Hong *et al.*, "Electroactive bio-composite actuators based on cellulose acetate nanofibers with specially chopped polyaniline nanoparticles through electrospinning," *Compos. Sci. Technol.*, vol. 87, pp. 135–141, 2013.
28. L. Montero de Espinosa, W. Meesorn, D. Moatsou, and C. Weder, "Bioinspired Polymer Systems with Stimuli-Responsive Mechanical Properties," *Chem. Rev.*, vol. 117, no. 20, pp. 12851–12892, Oct. 2017.
29. M. Mazurek-Budzyńska, M. Y. Razzaq, K. Tomczyk, G. Rokicki, M. Behl, and A. Lendlein, "Poly(carbonate-urea-urethane) networks exhibiting high-strain shape-memory effect," *Polym. Adv. Technol.*, vol. 28, no. 10, pp. 1285–1293, 2017.
30. R. C. P. Verpaalen, T. Engels, A. P. H. J. Schenning, and M. G. Debije, "Stimuli-Responsive Shape Changing Commodity Polymer Composites and Bilayers," *ACS Appl. Mater. Interfaces*, vol. 12, no. 35, pp. 38829–38844, Sep. 2020.
31. Q. M. Zhang and M. J. Serpe, "Stimuli-Responsive Polymers for Actuation," *ChemPhysChem*, vol. 18, no. 11, pp. 1451–1465, Jun. 2017.
32. N. K. Guimard, N. Gomez, and C. E. Schmidt, "Conducting polymers in biomedical engineering," *Prog. Polym. Sci.*, vol. 32, no. 8, pp. 876–921, 2007.
33. Y. Xia, Y. He, F. Zhang, Y. Liu, and J. Leng, "A Review of Shape Memory Polymers and Composites: Mechanisms, Materials, and Applications," *Adv. Mater.*, vol. 33, no. 6, p. 2000713, Feb. 2021.
34. A. Al-Abduljabbar and I. Farooq, "Electrospun Polymer Nanofibers: Processing, Properties, and Applications," *Polymers*, vol. 15, no. 1. 2023.
35. Z.-M. Huang, Y.-Z. Zhang, M. Kotaki, and S. Ramakrishna, "A review on polymer nanofibers by electrospinning and their applications in nanocomposites," *Compos. Sci. Technol.*, vol. 63, no. 15, pp. 2223–2253, 2003.
36. S. Y. Severt, S. L. Maxwell, J. S. Bontrager, J. M. Leger, and A. R. Murphy, "Mimicking muscle fiber structure and function through electromechanical actuation of electrospun silk fiber bundles," *J. Mater. Chem. B*, vol. 5, no. 40, pp. 8105–8114, 2017.
37. A. W. Laramée, C. Lanthier, and C. Pellerin, "Electrospinning of Highly Crystalline Polymers for Strongly Oriented Fibers," *ACS Appl. Polym. Mater.*, vol. 2, no. 11, pp. 5025–5032, Nov. 2020.
38. C. Huang *et al.*, "Stimuli-responsive electrospun fibers and their applications," *Chem. Soc. Rev.*, vol. 40, pp. 2417–2434, 2011.
39. C. Gotti, A. Sensini, A. Zucchelli, R. Carloni, and M. L. Focarete, "Hierarchical fibrous structures for muscle-inspired soft-actuators: A review," *Appl. Mater. Today*, vol. 20, p. 100772, 2020.
40. I. H. Kim *et al.*, "Human-muscle-inspired single fibre actuator with reversible percolation," *Nat. Nanotechnol.*, vol. 17, no. 11, pp. 1198–1205, 2022.
41. L. Tynan, G. Naik, G. D. Gargiulo, and U. Gunawardana, "Implementation of the Biological Muscle Mechanism in HASEL Actuators to Leverage Electrohydraulic Principles and Create New Geometries," *Actuators*, vol. 10, no. 2, p. 38, Feb. 2021.
42. M. Sharabi, "Structural Mechanisms in Soft Fibrous Tissues: A Review," *Front. Mater.*, vol. 8, Jan. 2022.
43. M. J. Abrams, T. Basinger, W. Yuan, C.-L. Guo, and L. Goentoro, "Self-repairing symmetry in jellyfish through mechanically driven reorganization," *Proc. Natl. Acad. Sci.*, vol. 112, no. 26, pp. E3365–E3373, Jun. 2015.

44. L. C. T. Scorza and M. C. Dornelas, "Plants on the move: Towards common mechanisms governing mechanically-induced plant movements," *Plant Signal. Behav.*, vol. 6, no. 12, pp. 1979–1986, Dec. 2011.
45. E. Liscum, S. K. Askinosie, D. L. Leuchtman, J. Morrow, K. T. Willenburg, and D. R. Coats, "Phototropism: growing towards an understanding of plant movement.," *Plant Cell*, vol. 26, no. 1, pp. 38–55, Jan. 2014.
46. A. G. Volkov, M.-R. Pinnock, D. C. Lowe, M. S. Gay, and V. S. Markin, "Complete hunting cycle of *Dionaea muscipula*: Consecutive steps and their electrical properties," *J. Plant Physiol.*, vol. 168, no. 2, pp. 109–120, 2011.
47. G. B. Monshausen, S. J. Swanson, and S. Gilroy, "Touch Sensing and Thigmotropism," in *Plant Tropisms*, 2007, pp. 91–122.
48. M. Farhan *et al.*, "Artificial Tendrils Mimicking Plant Movements by Mismatching Modulus and Strain in Core and Shell," *Adv. Mater.*, vol. 35, no. 22, p. 2211902, Jun. 2023.
49. J. Li, A. Tian, Y. Sun, B. Feng, H. Wang, and X. Zhang, "The Development of a Venus Flytrap Inspired Soft Robot Driven by IPMC," *J. Bionic Eng.*, vol. 20, no. 1, pp. 406–415, 2023.
50. S. Scherzer, W. Federle, K. A. S. Al-Rasheid, and R. Hedrich, "Venus flytrap trigger hairs are micronewton mechano-sensors that can detect small insect prey.," *Nat. plants*, vol. 5, no. 7, pp. 670–675, Jul. 2019.
51. K. Kareklas, D. Nettle, and T. V. Smulders, "Water-induced finger wrinkles improve handling of wet objects," *Biol. Lett.*, vol. 9, no. 2, p. 20120999, Apr. 2013.
52. K. Song *et al.*, "Journey of water in pine cones," *Sci. Rep.*, vol. 5, no. 1, p. 9963, May 2015.
53. E. Reyssat and L. Mahadevan, "Hygromorphs: from pine cones to biomimetic bilayers," *J. R. Soc. Interface*, vol. 6, no. 39, pp. 951–957, Oct. 2009.
54. Y.-C. Chuang *et al.*, "Electrospinning of Aqueous Solutions of Atactic Poly(N-isopropylacrylamide) with Physical Gelation," *Gels*, vol. 8, no. 11, p. 716, Nov. 2022.
55. E. Schoolaert *et al.*, "Waterborne Electrospinning of Poly(N -isopropylacrylamide) by Control of Environmental Parameters," *ACS Appl. Mater. Interfaces*, vol. 9, no. 28, pp. 24100–24110, Jul. 2017.
56. S. Lee, M. Lee, and J. Lee, "Highly sensitive humidity-responsive actuator comprising aligned electrospun fibers containing metal–organic framework nanoparticles," *Sensors Actuators B Chem.*, vol. 332, p. 129520, Apr. 2021.
57. S. Jiang, F. Liu, A. Lerch, L. Ionov, and S. Agarwal, "Unusual and Superfast Temperature-Triggered Actuators," *Adv. Mater.*, vol. 27, no. 33, pp. 4865–4870, Sep. 2015.
58. Y. Xu, A. Aiji, and M.-C. Heuzey, "Tunable two-step shape and dimensional changes with temperature of a PNIPAM/CNC hydrogel," *Soft Matter*, vol. 18, no. 23, pp. 4437–4444, 2022.
59. L. Liu, S. Jiang, Y. Sun, and S. Agarwal, "Giving Direction to Motion and Surface with Ultra-Fast Speed Using Oriented Hydrogel Fibers," *Adv. Funct. Mater.*, vol. 26, no. 7, pp. 1021–1027, Feb. 2016.
60. T. Chen, H. Bakhshi, L. Liu, J. Ji, and S. Agarwal, "Combining 3D Printing with Electrospinning for Rapid Response and Enhanced Designability of Hydrogel Actuators," *Adv. Funct. Mater.*, vol. 28, no. 19, p. 1800514, May 2018.
61. X. Wei *et al.*, "A robust anisotropic light-responsive hydrogel for ultrafast and complex biomimetic actuation via poly(pyrrole)-coated electrospun nanofiber," *Chem. Eng. J.*, vol. 452, p. 139373, Jan. 2023.
62. D. O. Miranda, M. F. Dorneles, and R. L. Oréface, "One-step process for the preparation of fast-response soft actuators based on electrospun hybrid hydrogel nanofibers obtained by reactive electrospinning with in situ synthesis of conjugated polymers," *Polymer (Guildf.)*, vol. 200, p. 122590, Jun. 2020.
63. J. Shang, X. Le, J. Zhang, T. Chen, and P. Theato, "Trends in polymeric shape memory hydrogels and hydrogel actuators," *Polym. Chem.*, vol. 10, no. 9, pp. 1036–1055, 2019.
64. C. Löwenberg, M. Balk, C. Wischke, M. Behl, and A. Lendlein, "Shape-Memory Hydrogels: Evolution of Structural Principles To Enable Shape Switching of Hydrophilic Polymer Networks," *Acc. Chem. Res.*, vol. 50, no. 4, pp. 723–732, Apr. 2017.
65. X. Gu and P. T. Mather, "Water-triggered shape memory of multiblock thermoplastic polyurethanes (TPUs)," *RSC Adv.*, vol. 3, no. 36, pp. 15783–15791, 2013.
66. J. Y. Ang, B. Q. Y. Chan, D. Kai, and X. J. Loh, "Engineering Porous Water-Responsive Poly(PEG/PCL/PDMS Urethane) Shape Memory Polymers," *Macromol. Mater. Eng.*, vol. 302, no. 9, p. 1700174, Sep. 2017.
67. X. Wei *et al.*, "An Electrospinning Anisotropic Hydrogel with Remotely-Controlled Photo-Responsive Deformation and Long-Range Navigation for Synergist Actuation," *Chem. Eng. J.*, vol. 433, p. 134258, Apr. 2022.

68. L. Liu, H. Bakhshi, S. Jiang, H. Schmalz, and S. Agarwal, "Composite Polymeric Membranes with Directionally Embedded Fibers for Controlled Dual Actuation," *Macromol. Rapid Commun.*, vol. 39, no. 10, p. 1800082, May 2018.
69. K. Cho, D. Kang, H. Lee, and W.-G. Koh, "Multi-stimuli responsive and reversible soft actuator engineered by layered fibrous matrix and hydrogel micropatterns," *Chem. Eng. J.*, vol. 427, p. 130879, Jan. 2022.
70. W. Liu, Y. He, and J. Leng, "Humidity-Responsive Shape Memory Polyurea with a High Energy Output Based on Reversible Cross-Linked Networks," *ACS Appl. Mater. Interfaces*, vol. 15, no. 1, pp. 2163–2171, Jan. 2023.
71. L. Ren, B. Li, Z. Song, Q. Liu, L. Ren, and X. Zhou, "Bioinspired fiber-regulated composite with tunable permanent shape and shape memory properties via 3d magnetic printing," *Compos. Part B Eng.*, vol. 164, pp. 458–466, May 2019.
72. L. Ren, B. Li, Z. Song, Q. Liu, L. Ren, and X. Zhou, "3D printing of structural gradient soft actuators by variation of bioinspired architectures," *J. Mater. Sci.*, vol. 54, no. 8, pp. 6542–6551, Apr. 2019.
73. V. Salaris, A. Leonés, D. Lopez, J. M. Kenny, and L. Peponi, "Shape-Memory Materials via Electrospinning: A Review.," *Polymers (Basel)*, vol. 14, no. 5, Feb. 2022.
74. M. Zare, P. Davoodi, and S. Ramakrishna, "Electrospun Shape Memory Polymer Micro-/Nanofibers and Tailoring Their Roles for Biomedical Applications," *Nanomaterials*, vol. 11, no. 4. 2021.
75. Y. Xia, F. Zhang, L. Wang, Y. Liu, and J. Leng, "18 - Electrospun shape-memory polymer fibers and their applications," in *Woodhead Publishing Series in Composites Science and Engineering*, Y. Dong, A. Baji, and S. B. T.-E. P. and C. Ramakrishna, Eds. Woodhead Publishing, 2021, pp. 567–596.
76. Q. Zhang *et al.*, "Temperature-controlled reversible pore size change of electrospun fibrous shape-memory polymer actuator based meshes," *Smart Mater. Struct.*, vol. 28, no. 5, p. 055037, May 2019.
77. T. Sauter, K. Kratz, M. Farhan, M. Heuchel, and A. Lendlein, "Design and fabrication of fiber mesh actuators," *Appl. Mater. Today*, vol. 29, p. 101562, 2022.
78. V. Izraylit, M. Heuchel, K. Kratz, and A. Lendlein, "Non-woven shape-memory polymer blend actuators," *MRS Adv.*, vol. 6, no. 33, pp. 781–785, Oct. 2021.
79. S. N. Banitaba *et al.*, "Biopolymer-based electrospun fibers in electrochemical devices: versatile platform for energy, environment, and health monitoring," *Mater. Horizons*, vol. 9, no. 12, pp. 2914–2948, 2022.
80. L. Liu, W. Xu, Y. Ding, S. Agarwal, A. Greiner, and G. Duan, "A review of smart electrospun fibers toward textiles," *Compos. Commun.*, vol. 22, p. 100506, 2020.
81. X.-X. Wang, G.-F. Yu, J. Zhang, M. Yu, S. Ramakrishna, and Y.-Z. Long, "Conductive polymer ultrafine fibers via electrospinning: Preparation, physical properties and applications," *Prog. Mater. Sci.*, vol. 115, p. 100704, 2021.
82. U. Kosidlo *et al.*, "Nanocarbon based ionic actuators—a review," *Smart Mater. Struct.*, vol. 22, no. 10, p. 104022, 2013.
83. J. C. García-Gallegos, I. Martín-Gullón, J. A. Conesa, Y. I. Vega-Cantú, and F. J. Rodríguez-Macías, "The effect of carbon nanofillers on the performance of electromechanical polyaniline-based composite actuators," *Nanotechnology*, vol. 27, no. 1, p. 15501, 2016.
84. Y. Bar-Cohen and I. A. Anderson, "Electroactive polymer (EAP) actuators—background review," *Mech. Soft Mater.*, vol. 1, no. 1, p. 5, Dec. 2019.
85. Q. Deng, H. Jia, C. An, S. Wu, S. Zhao, and N. Hu, "Progress and prospective of electrochemical actuator materials," *Compos. Part A Appl. Sci. Manuf.*, vol. 165, p. 107336, 2023.
86. P. Martins, D. M. Correia, V. Correia, and S. Lanceros-Mendez, "Polymer-based actuators: back to the future," *Phys. Chem. Chem. Phys.*, vol. 22, no. 27, pp. 15163–15182, 2020.
87. W. Serrano-Garcia, I. Bonadies, S. W. Thomas, and V. Guarino, "New Insights to Design Electrospun Fibers with Tunable Electrical Conductive&Semiconductive Properties," *Sensors*, vol. 23, no. 3. 2023.
88. H. Zong *et al.*, "Designing function-oriented artificial nanomaterials and membranes via electrospinning and electro spraying techniques," *Mater. Sci. Eng. C*, vol. 92, pp. 1075–1091, 2018.
89. T. Blachowicz and A. Ehrmann, "Conductive Electrospun Nanofiber Mats," *Materials (Basel)*, vol. 13, no. 1, p. 152, Dec. 2019.
90. J. C. Bittencourt, B. H. de Santana Gois, V. J. Rodrigues de Oliveira, D. L. da Silva Agostini, and C. de Almeida Olivati, "Gas sensor for ammonia detection based on poly(vinyl alcohol) and polyaniline electrospun," *J. Appl. Polym. Sci.*, vol. 136, no. 13, p. 47288, 2019.

91. J. Zhang *et al.*, "The aligned core–sheath nanofibers with electrical conductivity for neural tissue engineering," *J. Mater. Chem. B*, vol. 2, no. 45, pp. 7945–7954, 2014.
92. S. H. Bhang *et al.*, "Electroactive Electrospun Polyaniline/Poly[(L-lactide)-co-(ϵ -caprolactone)] Fibers for Control of Neural Cell Function," *Macromol. Biosci.*, vol. 12, no. 3, pp. 402–411, 2012.
93. C. Chen *et al.*, "Electrically-responsive core-shell hybrid microfibers for controlled drug release and cell culture," *Acta Biomater.*, vol. 55, pp. 434–442, 2017.
94. A. Laforgue and L. Robitaille, "Production of Conductive PEDOT Nanofibers by the Combination of Electrospinning and Vapor-Phase Polymerization," *Macromolecules*, vol. 43, no. 9, pp. 4194–4200, 2010.
95. Y. A. Ismail, M. K. Shin, and S. J. Kim, "A nanofibrous hydrogel templated electrochemical actuator: From single mat to a rolled-up structure," *Sensors Actuators B Chem.*, vol. 136, no. 2, pp. 438–443, 2009.
96. J. Li, S. Vadahanambi, C.-D. Kee, and I.-K. Oh, "Electrospun Fullerene-Cellulose Biocompatible Actuators," *Biomacromolecules*, vol. 12, no. 6, pp. 2048–2054, 2011.
97. L. Qian *et al.*, "Nanocellulose-based electroactive actuators and their performance with various ions," *Cellulose*, vol. 30, no. 7, pp. 4455–4468, 2023.
98. M. Li, Y. Guo, Y. Wei, A. G. MacDiarmid, and P. I. Lelkes, "Electrospinning polyaniline-contained gelatin nanofibers for tissue engineering applications," *Biomaterials*, vol. 27, no. 13, pp. 2705–2715, 2006.
99. Y. A. Ismail, J. G. Martínez, A. S. Al Harrasi, S. J. Kim, and T. F. Otero, "Sensing characteristics of a conducting polymer/hydrogel hybrid microfiber artificial muscle," *Sensors Actuators B Chem.*, vol. 160, no. 1, pp. 1180–1190, 2011.
100. Y. A. Ismail *et al.*, "Electrochemical actuation in chitosan/polyaniline microfibers for artificial muscles fabricated using an in situ polymerization," *Sensors Actuators B Chem.*, vol. 129, no. 2, pp. 834–840, 2008.
101. S. Florczak *et al.*, "Melt electrowriting of electroactive poly(vinylidene difluoride) fibers," *Polym. Int.*, vol. 68, no. 4, pp. 735–745, Apr. 2019.
102. S. Aznar-Cervantes *et al.*, "Fabrication of conductive electrospun silk fibroin scaffolds by coating with polypyrrole for biomedical applications," *Bioelectrochemistry*, vol. 85, pp. 36–43, 2012.
103. Y. Lv, X. Ma, Y. Xu, H. Shu, and W. Jia, "Effect of carboxymethyl cellulose on the output force and electrochemical performance of sodium alginate ion electric actuator," *Sensors Actuators A Phys.*, vol. 339, p. 113269, 2022.
104. S. V. Ebadi, D. Semnani, H. Fashandi, B. Rezaei, and A. Fakhrali, "Gaining insight into electrolyte solution effects on the electrochemomechanical behavior of electroactive PU/PPy nanofibers: Introducing a high-performance artificial muscle," *Sensors Actuators B Chem.*, vol. 305, p. 127519, 2020.
105. S. V. Ebadi, D. Semnani, H. Fashandi, and B. Rezaei, "Synthesis and characterization of a novel polyurethane/polypyrrole-p-toluenesulfonate (PU/PPy-pTS) electroactive nanofibrous bending actuator," *Polym. Adv. Technol.*, vol. 30, no. 9, pp. 2261–2274, 2019.
106. V. Mottaghitlab, B. Xi, G. M. Spinks, and G. G. Wallace, "Polyaniline fibres containing single walled carbon nanotubes: Enhanced performance artificial muscles," *Synth. Met.*, vol. 156, no. 11, pp. 796–803, 2006.
107. T. Nezakati, A. Seifalian, A. Tan, and A. M. Seifalian, "Conductive Polymers: Opportunities and Challenges in Biomedical Applications," *Chem. Rev.*, vol. 118, no. 14, pp. 6766–6843, 2018.
108. T. F. Otero and J. G. Martínez, "Ionic exchanges, structural movements and driven reactions in conducting polymers from bending artificial muscles," *Sensors Actuators B Chem.*, vol. 199, pp. 27–30, 2014.
109. T. F. Otero, J. G. Martínez, and J. Arias-Pardilla, "Biomimetic electrochemistry from conducting polymers. A review: Artificial muscles, smart membranes, smart drug delivery and computer/neuron interfaces," *Electrochim. Acta*, vol. 84, pp. 112–128, 2012.
110. M. Beregoi *et al.*, "Electrochromic properties of polyaniline-coated fiber webs for tissue engineering applications," *Int. J. Pharm.*, vol. 510, no. 2, pp. 465–473, 2016.
111. M. Beregoi, A. Evangelidis, E. Matei, and I. Enculescu, "Polyaniline based microtubes as building-blocks for artificial muscle applications," *Sensors Actuators B Chem.*, vol. 253, pp. 576–583, 2017.
112. B. K. Gu, Y. A. Ismail, G. M. Spinks, S. I. Kim, I. So, and S. J. Kim, "A Linear Actuation of Polymeric Nanofibrous Bundle for Artificial Muscles," *Chem. Mater.*, vol. 21, no. 3, pp. 511–515, 2009.
113. C. V Fengel, N. P. Bradshaw, S. Y. Severt, A. R. Murphy, and J. M. Leger, "Biocompatible silk-conducting polymer composite trilayer actuators," *Smart Mater. Struct.*, vol. 26, no. 5, p. 55004, 2017.
114. S.-S. Kim and C.-D. Kee, "Electro-active polymer actuator based on PVDF with bacterial cellulose nano-whiskers (BCNW) via electrospinning method," *Int. J. Precis. Eng. Manuf.*, vol. 15, no. 2, pp. 315–321, 2014.

115. M. Beregoi, S. Beaumont, S. I. Jinga, T. F. Otero, and I. Enculescu, "Chemical sensing and actuation properties of polypyrrole coated fibers," *Smart Mater. Struct.*, vol. 31, no. 10, p. 105012, 2022.
116. M. Beregoi, A. Evanghelidis, V. C. Diculescu, H. Iovu, and I. Enculescu, "Polypyrrole Actuator Based on Electrospun Microribbons," *ACS Appl. Mater. Interfaces*, vol. 9, no. 43, pp. 38068–38075, 2017.
117. M.-C. Bunea, M. Beregoi, A. Evanghelidis, A. Galatanu, and I. Enculescu, "Direct and remote induced actuation in artificial muscles based on electrospun fiber networks," *Sci. Rep.*, vol. 12, no. 1, p. 13084, 2022.
118. J. K. Kwon, H. J. Yoo, and J. W. Cho, "Conducting core-sheath polyurethane-PEDOT nanofibres for conducting polymer actuator," *Int. J. Nanotechnol.*, vol. 10, no. 8/9, pp. 661–670, 2013.
119. M. Harjo, Z. Zondaka, K. Leemets, M. Järvekülg, T. Tamm, and R. Kiefer, "Polypyrrole-coated fiber-scaffolds: Concurrent linear actuation and sensing," *J. Appl. Polym. Sci.*, vol. 137, no. 14, p. 48533, Apr. 2020.
120. M. Beregoi, N. Preda, A. Evanghelidis, A. Costas, and I. Enculescu, "Versatile Actuators Based on Polypyrrole-Coated Metalized Eggshell Membranes," *ACS Sustain. Chem. Eng.*, vol. 6, no. 8, pp. 10173–10181, 2018.
121. C. Gotti, A. Sensini, G. Fornaia, C. Gualandi, A. Zucchelli, and M. L. Focarete, "Biomimetic Hierarchically Arranged Nanofibrous Structures Resembling the Architecture and the Passive Mechanical Properties of Skeletal Muscles: A Step Forward Toward Artificial Muscle," *Front. Bioeng. Biotechnol.*, vol. 8, Jul. 2020.
122. Q. He *et al.*, "Electrospun liquid crystal elastomer microfiber actuator," *Sci. Robot.*, vol. 6, no. 57, p. eabi9704, 2021.
123. C. Lowenberg, M. Balk, C. Wischke, M. Behl, and A. Lendlein, "Shape-Memory Hydrogels: Evolution of Structural Principles To Enable Shape Switching of Hydrophilic Polymer Networks," *Acc Chem Res*, vol. 50, no. 4, pp. 723–732, 2017.
124. T. D. Brown, P. D. Dalton, and D. W. Hutmacher, "Melt electrospinning today: An opportune time for an emerging polymer process," *Prog. Polym. Sci.*, vol. 56, pp. 116–166, 2016.
125. H. El-Sayed *et al.*, "A critique on multi-jet electrospinning: State of the art and future outlook," *Nanotechnol. Rev.*, vol. 8, no. 1, pp. 236–245, 2019.
126. J. Lee, S. Moon, J. Lahann, and K. J. Lee, "Recent Progress in Preparing Nonwoven Nanofibers via Needleless Electrospinning," *Macromol. Mater. Eng.*, p. 2300057, 2023.

Disclaimer/Publisher's Note: The statements, opinions and data contained in all publications are solely those of the individual author(s) and contributor(s) and not of MDPI and/or the editor(s). MDPI and/or the editor(s) disclaim responsibility for any injury to people or property resulting from any ideas, methods, instructions or products referred to in the content.